Lehigh University
Lehigh Preserve

Theses and Dissertations

1-1-1982

The fracture behavior of A737 Grade B microalloyed steel weldment.

Jose Maria Aurrecoechea

Follow this and additional works at: http://preserve.lehigh.edu/etd

Part of the Materials Science and Engineering Commons

Recommended Citation

THE FRACTURE BEHAVIOR OF

A737 GRADE B MICROALLOYED STEEL WELDMENT

by

Jose Maria Aurrecoechea

A Thesis

Presented to the Graduate Committee

of Lehigh University

in Candidacy for the Degree of

Master of Science

in

Metallurgy and Materials Engineering

Lehigh University

1982

ProQuest Number: EP76229
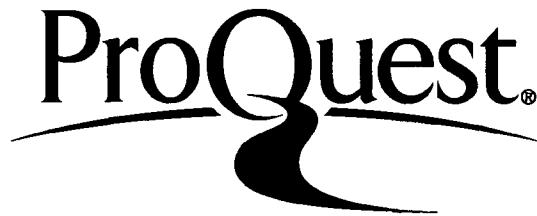
ProQuest.

ProQuest EP76229

CERTIFICATE OF APPROVAL

This thesis is accepted and approved in partial fulfillment of the requirements for the degree of Master of Science.

2 April 1982
(Date)

_____
Professor in Charge

_____
Chairman of Department

ii

ACKNOWLEDGEMENTS

TABLE OF CONTENTS

LIST OF TABLES

LIST OF FIGURES

ABSTRACT

A research program was conducted on a microalloyed steel weldment to provide information on the mechanical behavior of the weld metal and heat affected zone (HAZ). The effect of stress relief on the mechanical properties was also investigated. The weldment consisted of two 100mm (4 in.) thick plates of A737 Grade B Nb treated steel welded together with Armco W-19 wire and Linde 709-5 flux.

The tensile properties of the weld metal were measured at temperatures ranging between -75°C (-103°F) and 22°C (72°F). Charpy impact tests were run over a temperature range from -125°C (193°F) to 22°C (72°F). The Nil-Ductility Transition Temperature was determined. The static fracture toughness and dynamic fracture toughness were evaluated at 22°C (72°F) and 50°C (-58°F).

The cross weld tensile test results showed that the room temperature tensile strength decreased from 636 MPa (92.2 Ksi) to 573 MPa (83.0 Ksi) with a 10 hour post-weld stress relief treatment at 593°C (1100°F). However, the weld metal overmatched the strength of the base plate even after the post-weld heat treatment. Charpy impact test results indicated that the toughness of the weld metal was lower than that of the HAZ which in turn was slightly lower than that of the base plate. The Charpy impact toughness of both the weld metal and HAZ improved slightly with post-weld heat treatment. Drop weight tests performed on the weld metal supported this observation.

1

The static fracture toughness test results confirmed that the HAZ was tougher than the weld metal for every stress relief condition. The toughness of both regions increased with temperature. The dynamic fracture toughness of the weld metal exhibited a similar behavior.

From all the test results it can be concluded that the weldment possessed an adequate combination of toughness and strength. The balance of mechanical properties was not substantially modified by the post-weld stress relief treatment.

INTRODUCTION

Background

Progress in science and technology has always been closely associated with the development of new materials and such has been the case of the pressure vessel industry. Over the years, new design methods and new materials requirements have produced new property evaluation techniques and a number of new pressure vessel steels.[1]

The development of a new pressure vessel steel is never complete until all its properties have been carefully examined. Such an investigation will include the evaluation of strength, toughness over a certain temperature range, weldability, formability, fatigue behavior, creep resistance, response to heat treatment, and the effect of operating environment on these properties. Once the characteristics of the steel become known, it is possible to compare it with existing steels and determine the limits of its application.

In response to this necessity, the Pressure Vessel Research Committee (PVRC) of the Welding Research Council began in 1972 to sponsor research programs aimed to developing mechanical property data for promising pressure vessel steels. Attention was given to a group of microalloyed steels adopted for pressure vessel use under ASTM specification A737. This specification covers grades A (Vanadium treated), B (Niobium treated), and C (Vanadium and Nitrogen treated). Over the past few years, work at Lehigh University has focussed on the mechanical behavior of grades B and C. Property related characteristics including fracture toughness[2,3],

3

effect of stress relief[4], and susceptibility to strain aging[5,6]
have been assessed.

The next phase of this work would be to determine the weld-
ability of these steels. With this in mind, the fracture toughness
of an A737B microalloyed steel weldment has been studied under PVRC
sponsorship and the results are reported here. Since base plate
properties were developed in previous work at Lehigh, these same
steels were used to develop weld metal and HAZ data. Primary
emphasis is, therefore, on properties of the weldment, but comparison
is made to base plate data when appropriate.

Niobium Treated Microalloyed Steels

A737B belongs to a group of materials called microalloyed
steels. These steels are included in the much larger designation
of high-strength low-alloy (HSLA) steels although their strength
levels are only moderate. Microalloyed steels constitute the most
recent development in steels for pressure vessel service. These
steels are well suited for applications where good low temperature
toughness, moderate strength, adequate weldability and low cost
are required. Another group of steels included in the HSLA desig-
nation are the dual-phase (ferritic-martensitic) steels. Their
strength, toughness, and excellent formability make them very
promising for automobile applications [7-9].

The beginning of HSLA steels can be traced to the early 1900's
according to Pickering. [10]   Steady progress has been achieved
through the years, in producing steels of higher strength balanced

4

by good toughness through laboratory studies of microstructure-property relationships and improvements in steelmaking processes. In 1947 Barr and Honeyman determined that an increase in the manganese to carbon ratio in these steels produced a finer grain steel which in turn was responsible for a decrease in the impact transition temperature.[11] Several years later, it was also discovered that ferrite-grain refinement had a beneficial effect on the yield strength. [12,13] Once these facts became known, normalized fine grained steels of superior strength and toughness were introduced to the market.

Initially, grain refining was done with aluminum with or without nitrogen but later other additives such as niobium, vanadium, and titanium were found to provide the same effects. Niobium was specially attractive because very small amounts produced remarkable strengthening through grain refinement. In 1958, Great Lakes Steel Corporation began to market the first niobium treated steels under the GLX-W designation. [14] These steels had 0.14 to 0.20% carbon, 0.40 to 1.00% manganese, and 0.01 to 0.03% niobium, and were produced in hot rolled plate with yield strengths up to 415 MPa (60 ksi).

At this stage, it was only known that niobium was a very potent ferrite-grain refiner. A few years later Morrison and Woodhead [15] pointed out that the marked strengthening effect of small additions of niobium could not be fully explained by grain refinement alone, as described by the Petch relationship. [13] In addition, they also

5

observed an increase in impact transition temperature which could not be explained. Furthermore, at any fixed grain size, the strength and impact transition temperature increased with larger amounts of niobium. The authors suggested that, due to the affinity of niobium for carbon and nitrogen, the increase in strength could be caused by precipitates of niobium carbide, nitride, or a mixed compound.

Shortly after, Morrison proved that the presence of niobium carbide or nitride was partly responsible for the increase in strength. [16] It was also concluded that grain refinement was the main source of strengthening by niobium in steels austenitized at temperatures below 1050°C whereas steels austenitized at higher temperatures (1200°C) were strengthened by precipitation hardening by a niobium carbide or nitride. Irvine and Pickering arrived at the same conclusions. [17]

At that time, the impact properties of niobium steels were not good because of their coarse as-rolled austenite grain size. Making use of the knowledge acquired Irvine et al suggested that adequate control of the rolling variables and the heating and cooling cycles could solve the problem. [18] Consequently two possibilities were considered:

1. Controlled rolling at a low finishing temperature: This would produce a fine austenite and consequently a fine-ferrite grain sized steel, with some precipitation strengthening effect.

6

2. Normalizing: If controlled rolling is not practicable, a normalizing treatment may be necessary. The austenitizing temperature has to be low enough to assure a fine austenite grain size and as a result a fine grained ferritic structure can be obtained.

A problem that persisted was the presence of elongated stringers of manganese sulphide inclusions parallel to the rolling direction. These inclusions were the cause of poor toughness in the through-thickness direction of hot rolled plates, and as a result, toughness and ductility were highly anisotropic. An important achievement in this field has been inclusion-shape control. [10] It was discovered that the addition of certain elements such as zirconium [19], cerium [20], or calcium [21] reduced the plasticity of the inclusions which, therefore, could not become elongated due to the rolling operation.

In recent years, improvements have continued in the field of HSLA steels in general and niobium treated microalloyed steels in particular. Extensive research has been done to fully understand the role of the niobium addition in these steels. [22,23] This knowledge has been very useful in designing new steels.

One such steel, A737B, is designed in response to the need for an economical carbon steel with good strength and superior low temperature toughness. [24,25] No controlled rolling is necessary because the plates are heat treated after conventional rolling. The plates can be either quenched and tempered or normalized. The latter is the case of the material used in the weldment studied.

The critical variable in the heat treatment operation is the austenitizing temperature.

The steel contains niobium carbonitride precipitates in the as-rolled condition. The solubility of niobium carbonitride in austenite is a function of temperature. If the austenitizing temperature is high, around 1250°C, the precipitates will dissolve and austenite grain coarsening occurs. On cooling, coarse ferrite forms and the carbonitrides reprecipitate due to their low solubility in ferrite. The result is a dispersion hardened coarse grained ferrite-pearlite steel. This microstructure is undesirable because of its low toughness.

On the other hand, austenitizing at a low temperature (900°C) produces a different effect. At this temperature, the niobium carbonitride precipitates do not dissolve in the austenite and, therefore, inhibit grain growth. Consequently a fine grained ferrite-pearlite steel forms after cooling. The beneficial effects of grain refinement on toughness and strength are thus obtained. At intermediate austenitizing temperatures both behaviors are observed. Therefore, A737B steel is austenitized at 900°C and normalized.

Weldability of Microalloyed Steels

Weldability is a property that has to be evaluated before a steel for pressure vessel service can be utilized. It may be defined as the ease with which required performance characteristics can be obtained from a joint with a given set of welding

conditions.[23] Weldability is a complex property and two aspects
have to be considered, fabrication weldability and service weld-
ability.[1]

Fabrication Weldability

Arc welding is the process most frequently used to join steels
for pressure vessel applications. From the fabrication weldability
aspect, three problems have to be considered. They are hydrogen
induced cracking, solidification cracking and lamellar tearing.

Hydrogen induced cracking or cold cracking is the most
important source of welding defects. It takes place mainly in the
HAZ but it can also appear in the weld metal. Cracking can occur
from a combination of an unfavorable HAZ microstructure, presence
of hydrogen and an applied stress. The susceptibility to cold
cracking depends on the presence of martensite in the HAZ. A
convenient way to assess the tendency to form martensite is the
concept of carbon equivalent (CE). The CE formula can take many
forms. The formula that appears in the A737 specification is as
follows:

$$CE = C + \frac{Mn + Si + Cr + Mo}{6} + \frac{Ni + Cu}{16}$$

where the numbers for the elements are the alloy contents in
weight percent. As observed in the formula, niobium does not seem
to have any significant effect.[26]

It has been observed empirically that cold cracking seldom
occurs if the hardness of the HAZ is below 30Rc.[27] This can be
achieved by decreasing the carbon content or by reducing the

9

cooling rate following welding. The usage of preheat can effectively reduce the cooling rate, and thus help avoid hydrogen induced cracking.

Solidification cracking or hot cracking occurs in the weld metal and has been related to segregation during solidification. The most common cause is the presence of low-melting iron and alloy sulfides in the weld metal.[23] Phosphorus and sulfur are strong promoters of hot cracking. Cracking can be avoided by controlling the amount and types of sulfides. This is done by using a specified manganese to sulfur ratio depending on the carbon content.

Lamellar tearing is a defect in the base metal caused by shrinkage forces in the plate thickness direction. This problem can be encountered in highly restrained joints. The occurrence of lamellar tearing has been linked to the presence of manganese sulfide inclusion stringers or plates in the rolling direction. These elongated inclusions produce low toughness in the short transverse direction. Sulfide inclusion shape control can be used to minimize the possibility of lamellar tearing. Recently, hydrogen and arc contamination have also been identified as promoters of lamellar tearing.[28]

Service Weldability

From the service weldability viewpoint, the main concern is to obtain a joint with an optimum balance of properties. Therefore, careful attention has to be given to the toughness of the

10

HAZ and the weld metal, as well as the strength of the weldment.

The HAZ is a complex microstructural composite. Different peak temperatures reached during the welding operation produce a variety of structures in different regions of the HAZ. The complexity increases in the case of multipass welds. The coarse grained region of the HAZ possesses the lowest toughness. Research has shown that niobium has little effect on the toughness of the HAZ at low weld heat inputs but at higher inputs it has a detrimental effect.[26] Experiments have revealed that the loss of toughness is due to the formation of predominantly upper bainitic structures of high hardness.[29] No niobium carbonitrides were observed in the HAZ by this investigator but another researcher reports that there are.[30] Therefore, there still is no consensus over the role of niobium in the HAZ.

The toughness of the weld metal is also important. It depends mainly on the composition and the process variables. The weld metal usually has a lower carbon content than the base metal. Nickel is sometimes added to increase the weld metal toughness. This is the case of the Armco W-19 used in this investigation. The strength of the weldment is another property that concerns the manufacturer and the user. In the case of microalloyed steels, the weld metal often is stronger than the base plate. Such is the case of the weldment studied.

There are several thermal and mechanical treatments performed on weldments to reduce residual stresses and distortion. These

11

HAZ and the weld metal, as well as the strength of the weldment.

The HAZ is a complex microstructural composite. Different peak temperatures reached during the welding operation produce a variety of structures in different regions of the HAZ. The complexity increases in the case of multipass welds. The coarse grained region of the HAZ possesses the lowest toughness. Research has shown that niobium has little effect on the toughness of the HAZ at low weld heat inputs but at higher inputs it has a detrimental effect.[26] Experiments have revealed that the loss of toughness is due to the formation of predominantly upper bainitic structures of high hardness.[29] No niobium carbonitrides were observed in the HAZ by this investigator but another researcher reports that there are.[30] Therefore, there still is no consensus over the role of niobium in the HAZ.

The toughness of the weld metal is also important. It depends mainly on the composition and the process variables. The weld metal usually has a lower carbon content than the base metal. Nickel is sometimes added to increase the weld metal toughness. This is the case of the Armco W-19 used in this investigation. The strength of the weldment is another property that concerns the manufacturer and the user. In the case of microalloyed steels, the weld metal often is stronger than the base plate. Such is the case of the weldment studied.

There are several thermal and mechanical treatments performed on weldments to reduce residual stresses and distortion. These

11

treatments often alter the mechanical properties of the weldment. A post-weld stress relief is one such treatment. It has a tempering effect on any martensite that might have formed in the HAZ and thus prevents cold cracking. However, in the case of niobium treated steels, the toughness of the HAZ decreases after post-weld heat treatment (PWHT) due to the hardening effect produced by the precipitation of niobium carbonitrides.[30] Therefore, the overall change in toughness will depend on which of the two effects predominates at the heat input used. PWHT is more beneficial at low heat inputs than at high heat inputs. There is also the possibility of stress relief cracking, but this has not been an important problem for microalloyed steels.[31]

The influence of PWHT on the mechanical properties of the weld metal is also important. The heat treatment usually softens the weld metal in steel weldments. The toughness may or may not increase depending on the composition and as welded structure of the weld metal.

Fracture Mechanics

The first fracture toughness test emerged in the 1940's when the Charpy impact test was used to evaluate the toughness of ship plate. In 1952 another method, the Nil-Ductility Transition Temperature (NDTT) test, was developed at the Naval Research Laboratory. Over the years, both tests have been utilized extensively due to their relative simplicity and inexpensiveness and now are standard procedures described in ASTM specifications E23 and E208. Both

tests measure the resistance to fracture under impact loading in the presence of a stress concentration, but are essentially empirical and largely qualitative in nature.

More recently, the principles of Linear Elastic Fracture Mechanics (LEFM) have been developed and used for determining fracture toughness. The outcome is a test method for measuring plane strain fracture toughness (K_{1C}) outlined in ASTM specification E399. The fracture toughness (K_c) is a material property that depends on specimen thickness. When the thickness increases, plane strain conditions prevail and the fracture toughness drops to a lower value (K_{1C}) that does not decrease further with increasing thickness. Therefore, K_{1C} is a conservative lower limit value of fracture toughness that can be used for design purposes. This represents a great improvement over the Charpy and NDTT tests because it can be used to limit stress and control brittle fracture.

However, the use of LEFM is limited to high strength materials which have little or no plastic deformation prior to failure. As a result the fracture behavior of pressure vessel steels, with their high toughness and moderate strength, cannot be accurately described with this analysis.

In addition, plane strain conditions must exist during the test in order to obtain K_{1C}. This is accomplished only when the following inequality is fulfilled

$$B \geq 2.5 \left(\frac{K_{1C}}{\sigma_{ys}}\right)^2 \qquad (1)$$

13

where B is the specimen thickness and σ_{ys} the yield strength of the material. The thickness of pressure vessel steel specimens would have to be very large (200mm or more). The testing of specimens of such size is impractical and prohibitively expensive.

It was necessary to develop a new approach to describe the fracture conditions of a material experiencing both elastic and plastic deformation. One approach was the concept of the J integral proposed by Rice in 1968.[32] It is defined by

$$J = \int_{\Gamma} (W dy - T \frac{\partial u}{\partial x} ds) \qquad (2)$$

where

$$W = W(x,y) = W(\varepsilon) = \int_{0}^{\varepsilon} \sigma_{ij} \, d\varepsilon_{ij} \qquad (3)$$

Here W is the strain energy density, Γ is any given curve surrounding the notch tip, T is the traction vector, u is the displacement vector, ds is an element of arc length along Γ, σ_{ij} is all stresses in a two dimensional deformation field, ε is the infinitesimal strain tensor, and x,y are the rectangular coordinates normal to the crack front.

Furthermore, Rice proposed an alternate and equivalent definition for the J integral. He defined it as the potential energy difference between two identically loaded bodies possessing slightly different crack lengths and so

$$J = - \frac{dU}{da} \qquad (4)$$

where U is the potential energy and a is the crack length. For

14

elastic-plastic materials, J becomes a measure of the characteristic elastic-plastic stress-strain field surrounding the crack tip.[33]

Landes and Begley made use of equation 4 to experimentally determine J_{1C} but their method was tedious and often difficult. More recently, Rice et al proposed a simpler method to experimentally measure the J integral.[34] J is calculated using a load-load line displacement curve from the test record. Here:

$$J = \frac{2A}{Bb}, \qquad (5)$$

where A is the area under the load-load line displacement curve, B is the specimen thickness and b is the unbroken ligament remaining after testing. Equation 5 defines J for a three-point bend specimen with a span/width ratio of four. To account for the presence of a tensile loading component in the compact tension specimen, Merkle and Corten[35] suggested a modification to equation 5,

$$J = \frac{2A}{Bb} \left(\frac{1 + \alpha}{1 + \alpha^2} \right), \qquad (6)$$

where

$$\alpha = \left[\left(\frac{2a_0}{b} \right)^2 + 2 \left(\frac{2a_0}{b} \right) + 2 \right]^{\frac{1}{2}} - \left(\frac{2a_0}{b} + 1 \right), \qquad (7)$$

and where ao is the initial crack size. For large crack lengths (a/w > 0.6, where w is the specimen width), equations 5 and 6 approach one another.

Landes and Begley[36] proposed that J_{1C} could be determined by measuring J values from several specimens which had undergone different amounts of crack extension, Δa. These J values are plotted

15

versus the crack extension and a crack resistance R-curve can be obtained. The J_{1C} value is then defined at some location on the J-Δa curve corresponding to the point of first crack advance. This location is determined by the intersection of the R-curve with the so-called "blunting line",

$$J = 2 \sigma_{flow} \Delta a , \qquad (8)$$

where σ_{flow} is the average of the yield and tensile strength of the material.

The J integral testing method has not yet been standardized in an ASTM specification. However, Clarke et al[37] have published a recommended procedure, introducing some limitations to insure reliable data. The maximum load during precracking of the test specimens must not exceed one fourth P_L to minimize the plastic zone introduced during precracking. P_L is calculated by

$$P_L = \frac{B \ b^2 \ \sigma_{flow}}{2w + a} \qquad (9)$$

for compact tension specimens, and

$$P_L = \frac{4}{3} \ \frac{B \ b^2 \ \sigma_{flow}}{S} \qquad (10)$$

for three point bend specimens, where S is the span. As such, this criterion is more restrictive than the one in ASTM E399.

The blunting line is calculated using equation 8, and two offset lines are constructed parallel to the blunting line and intersecting the x-axis at 0.15mm and 1.5mm. Only the J values located between these lines can be used to determine J_{1C} and a

16

minimum of four values are needed. The R-curve is constructed by a least squares fit of the J values.

The specimens must also meet the following size requirements

$$B > \frac{25J_Q}{\sigma_{flow}} \qquad (11)$$

and

$$b > \frac{25J}{\sigma_{flow}} \qquad (12)$$

where J_Q is the intersection of the blunting line and the R-curve and J is the value of each specimen according to equation 6. If these criteria are met, $J_Q = J_{1C}$. These specimen size restrictions are much less severe than that of E399.

If no significant crack extension occurs before failure, the area under the load-load line displacement trace up to maximum load is used in equation 6 and this value is considered to be J_{1C}. An average of 3 values are needed to calculate J_{1C}. Once the J_{1C} value is known, it can be converted to K_{1C} for purposes of comparison. This may be done using an expression proposed by Begley and Landes.[33]

$$K_{1C} = \left(\frac{J_{1C} \, E}{1 - \nu^2} \right)^{\frac{1}{2}} \qquad (13)$$

where E is Young's elastic modulus and ν is Poisson's ratio.

Nonetheless, J_{1C} as defined corresponds to zero crack extension while K_{1C} corresponds to up to 2% crack extension. J_{1C} and K_{1C} should agree well for the case of a brittle material with a shallow R-curve but in the case of a tough material with a steep

17

R-curve the agreement is not as good. In such a case, J_{1C} is an even more conservative fracture toughness value than K_{1C}. This is because J_{1C} does not account for the ability of a tough material to withstand a certain amount of stable crack growth prior to failure.

Paris et al[38] have proposed that the slope of the R-curve can be used to determine a material constant which they have called the tearing modulus

$$T = \left(\frac{dJ}{da} \right) \frac{E}{\sigma_o^2} \qquad (14)$$

where dJ/da is the slope of the $J-\Delta a$ curve and σ_o (or σ_{flow}) is the average of the yield strength and tensile strength. Assuming an elastic-ideally plastic behavior, Paris et al[38] established that for stability, T had to be larger than a certain critical value dependant only on specimen geometry. However, results obtained by Landes and Begley[39] seem to indicate that T may also depend on specimen configuration. More work is being done to determine the general applicability of this new parameter.

For materials that display strain rate sensitivity, fracture toughness measured under conditions of dynamic loading may be a more important property than the static fracture toughness.[40] The dynamic fracture toughness is not easy to measure because the high strain rates produced by impact loads are difficult to record. Furthermore, the definition of the onset of crack propagation is often uncertain.

18

The critical strain energy release rate (J_{Cd}) is calculated by dropping an instrumented impact load on a fatigue precracked three-point bend specimen of the type specified in ASTM E399. Strain gages attached to the impacting tip measure the load transferred to the test specimen and so a load-time trace can be plotted on an x-y recorder. The velocity of the impacting tup when it strikes the specimen can be measured by

$$Vo = (2gh)^{\frac{1}{2}} \qquad (15)$$

where g is the gravitational constant and h is the height from which the weight is dropped. Once Vo is known, the energy required for failure (Wm) can be determined by the expression

$$Wm = Vo \int_0^{tm} Pdt \qquad (16)$$

where $\int_0^{tm} Pdt$ is the area under the load-time trace up to maximum load. This load is associated with crack initiation for the lack of a better starting point.

The dynamic fracture toughness can be calculated from the energy to failure by

$$K_{Cd} = (E\ J_{Cd})^{\frac{1}{2}} = \left(\frac{2\ WmE}{Bb} \right)^{\frac{1}{2}} \qquad (17)$$

J_{Cd} has a limited meaning since crack initiation is not well defined and J_{Cd} does not include inertial effects associated with dynamic behavior.[40]

Shoemaker and Rolfe[41] have proposed that the fracture resistance of steels having different yield strengths can be compared using

19

the K_{1C}/σ_{ys} ratio. This ratio appears in equation 1 and is a measure of the plate thickness necessary for plane strain conditions at fracture, which in turn is related to the plastic zone size at the crack tip during fracture. Therefore, steels with a large K_{1C}/σ_{ys} ratio possess good failure resistance. In addition, steels with similar ratios should have similar fracture resistance, regardless of yield strength. The ratio for dynamic properties K_{dt}/σ_{yd} can also be used for comparative purposes.

Experimental Objectives

The main objective of this investigation was to evaluate the mechanical properties of an A737 Grade B microalloyed steel weldment. Testing included tension, Charpy impact and NDTT tests. However, the emphasis was on fracture toughness characterization using J integral techniques. Additionally, the effect of a postweld stress relief heat treatment on the mechanical behavior of the weld metal and HAZ was also studied.

MATERIALS AND PROCEDURES

Materials

The microalloyed steel plates used in this investigation were supplied by Lukens Steel Company. The steel is Lukens low sulfur "frostline" grade and it meets the specification for A737 grade B. The chemical composition and mechanical properties were determined by Lukens and are given in Table 1.

The steel was produced in an electric arc furnace using a cold scrap charge, and subsequently calcium treated for desulfuration to 0.010% S maximum and inclusion shape control. Rolling was done by conventional practices. The plates were austenitized at 900°C (1650°F) and cooled in still air.

The filler metal used to fabricate the weldment was Armco W-19 4mm (0.156 in.) diameter wire. Its chemical composition is shown in Table 1.

Welding Operation

The A737 grade B plates were welded with Armco W-19 wire and Linde 709-5 flux. All the materials and weld parameters were selected to furnish a joint with good toughness and adequate strength. Armco W-19 is a low carbon filler metal with 3.5% nickel for added toughness. On the other hand, Linde 709-5 is a neutral flux formulated to provide a high toughness weld. Its composition is in Table 1.

The weldment was made using the submerged arc process. A direct current reverse polarity type arc was utilized. Using

21

a current intensity of 550A, a voltage of 32V, and a travel speed of 381 mmpm (15 inpm), a heat input of 2.77 KJmm^{-1} (70.4 KJin^{-1}) was produced. Preheat for the welding operation was 93°C (200°F) and the maximum interpass temperature was 149°C (300°F).

A double bevel was machined on one of the plates and a "K" groove was used as shown in Figure 1. This was done to obtain a straight HAZ and thus facilitate specimen preparation and mechanical testing. 81 passes were necessary to complete the weld which was oriented parallel to the rolling direction of the plates. Welding was done at Lukens Steel Corporation.

Stress Relief

The post-weld stress relief heat treatment was performed at 593°C (1100°F) for two and ten hours in a Hevi-duty forced air furnace. The material was then furnace cooled at a rate of 30°C (86°F) per hour down to 250°C (482°F) and subsequently air cooled from this temperature.

Specimen Layout

The welded plate measured approximately 102mm x 940mm x 1397mm (4 in. x 27 in. x 55 in.). The orientation of the plate with respect to the rolling direction can be seen in Figure 2. The plate was cut according to Figure 2 in order to obtain 17 pieces with dimensions 102mm x 406mm x 76 mm (4 in. x 16 in. x 3 in.). The different mechanical test specimens were machined from these these pieces as shown in Figure 3.

Hardness Testing

Hardness tests were done on a 102mm x 406mm x 76mm piece using a Wilson Rockwell hardness tester. Measurements were taken at regular intervals across the weld. Care was exercised to insure that the specimen would remain steady during the test. A portable jack was used for this purpose.

Tension Testing

Standard 6.35mm (0.25 in.) diameter buttonhead tension specimens were machined from the weld metal transverse to the welding direction. As seen in Figure 3, the specimens had to be taken from the surface ends of the welds to assure that the entire reduced section containing the 25.4mm (1 in.) gage length consisted exclusively of weld metal. Testing was done according to ASTM specification E8.

The ambient temperature tests were performed using a 44.5kN (10,000 lb) capacity Instron Universal Tester. A crosshead speed of 1.27mmpm (0.05 inpm) was used. An extensometer was employed to measure elongation to past the yield point and a load-displacement trace was obtained on an x-y recorder. The specimens were tested to failure.

The low temperature tests were run on the same testing machine. The specimens were immersed in a mechanically stirred methanol bath cooled by liquid nitrogen during testing. The temperature of the bath was monitored with a thermometer. The specimens were held at

23

temperature for 10 minutes prior to testing. No extensometer was used and the crosshead speed was also 1.27mmpm. The chart speed used was 50.8mmpm (2 inpm) and a load-displacement trace was recorded.

The 0.2% offset yield strength and ultimate tensile strength were calculated for all specimens. The elongation and reduction in area were determined by fitting together the two halves of the broken specimens and measuring final gage length and diameter with a vernier caliper.

Charpy Impact Testing

Standard type A impact specimens were machined from the weld metal and HAZ in the transverse (TL) orientation as shown in Figure 3. Testing was conducted on a certified calibrated Satec SI-1 impact testing machine, according to ASTM specification E23. A mechanically stirred bath of 2-methylbutane cooled by liquid nitrogen was used to achieve low temperature. The specimens were maintained at temperature for a minimum of five minutes before testing and were tested within five seconds after removal from the bath.

The impact energy of each specimen was recorded from the gage built into the machine and lateral expansion was measured using a dial gage along the edge of the broken specimens.

NDTT Testing

The nil-ductility transition temperature tests were performed

in accordance to ASTM specification E208. Five P3 specimens for each weld metal heat treatment condition were machined as seen in Figure 4. The orientation of the drop-weight specimens with respect to the weld can be observed in Figure 3. The crack starter welds were deposited using Murex-Hardex-N welding electrodes, 160A, 30V and a travel speed of 559mmpm (22 inpm). Subsequently, the weld beads were notched following the guidelines of E208.

Testing was done on a drop-weight test machine in Whitaker Laboratory at Lehigh. A 556 N (125 lb.) weight was dropped from a height of 732mm (28.8 in.) providing the required 400J (300 ft-lb) test energy. The specimens were cooled with liquid nitrogen in a mechanically stirred bath of 2-methylbutane. They were held at temperature for a minimum of 15 minutes before testing. The NDT temperature was determined by the specimen which failed at the highest temperature.

Static Fracture Toughness Testing

The static fracture toughness tests were done using a special double notched compact specimen so that the weld metal and HAZ could be tested with one specimen. These were machined in the transverse (TL) orientation. The configuration and dimensions of the specimens are shown in Figure 5. This modification does not alter the test results since the stress intensity factor, for the a/w values used, is essentially the same.[42]

In practice, the specimen is treated as two compact specimens

tested in sequence. Initially only two contiguous pin holes and
a notch are machined. The notch is fatigue cracked using the two
pinholes on either side of the notch. This portion of the specimen
is tested and after fracture, another pinhole and notch are
machined on the remaining larger portion of the specimen. The
result is essentially a standard compact specimen which is tested
in the same way as before.

All specimens were precracked on an Amsler Vibrophore fatigue
testing machine. Precracking was done using a 15.1kN (3400 lb)
load to initiate the crack. This load represents between 29 and
37% of the maximum loads (P_L) set by equation 9, which is in excess
of the 25% limit recommended. As the fatigue cracks grew, the
loads were progressively lowered and the recommended loads were
used for the final 3mm of crack length. This procedure was followed
because the use of the suggested loads did not produce crack
initiation.

Fracture toughness testing was performed on a 533kN (120,000 lb)
capacity Baldwin Universal Tester. Specimens were pulled in tension,
the load measured by a strain gage in the load cell and the crack
opening displacement measured by a clip-type strain gage set at the
face of the specimen. A Vishay amplifier and a Hewlett-Packard
x-y recorder were used to plot a load-face displacement trace as
seen in Figure 6.

The J integral techniques require determinations of area under
the load-load line displacement curve. Due to the specimen size,

26

it was impossible to measure load line displacements. Therefore, face line displacements were recorded and later converted to load line displacements using an equation derived from relationships formulated by Hollstein and Blauel.[43] The equation utilized was

$$\delta = \frac{[(1.25w^2 - 0.9bw - 11.6bv)^2 - 4(11.6b)(0.9bvw - vw)]^{\frac{1}{2}}}{23.2b}$$

$$+ \frac{(0.9bw - 1.25w^2 + 11.6bv)}{23.2b} \qquad (18)$$

where w is the width of the specimen, δ is the load line displacement and v is the face displacement.

Low temperature tests were conducted inside an insulated spray box which enclosed the specimen and clevis grips. Liquid nitrogen was sprayed directly on the specimen and temperature was measured by a copper-constantan thermocouple embedded within the specimen. All specimens were held at or below the test temperature for at least 15 minutes prior to testing.

The specimens which did not fail during the tests were heat tinted at 300°C (572°F) for one hour to mark the crack extension. These were then immersed in liquid nitrogen till cold and broken open on the Baldwin machine. The crack extension (Δa) was measured under a microscope, using a stage with a micrometric drive. An average of nine measurement points from one side of the specimen to the other across the crack front was used to calculate Δa. All other specimen dimensions were measured with a vernier caliper. After calculating the area under the load-load line displacement

trace the data was processed according to the recommended
procedure.[37]

Dynamic Fracture Toughness Testing

Standard 19mm (0.75 in.) thick three-point bend specimens were
machined in the transverse (TL) orientation. Figure 7 shows the
configuration and dimensions of the specimens. All specimens were
precracked on an Amsler Vibrophore apparatus, following the
procedure used for the compact tension specimens. The applied
loads for fatigue initiation never exceeded 40% of the maximum load
(P_L). In the final stage of fatigue crack growth, the loads
applied were 25% of P_L as recommended.[37]

Testing was conducted in Fritz Laboratory at Lehigh using a
drop-weight test facility adapted for three-point bend testing.
A 1.78 kN (400 lb) weight dropped from heights ranging from 305mm
(12 in.) to 610mm (24 in.) provided the striking force. Half-
round 13mm (0.5 in.) diameter rods were placed at the impact points
to cushion the impact and prevent ringing. After the specimen
fractures the falling weight is stopped by two aluminum blocks
which absorb the remaining energy in the weight.

The striking tup is instrumented and serves as the load
dynamometer. The load signal was recorded on a Tektronix Type 549
storage oscilloscope. When the weight is released, a shutter
attached to the drop-weight breaks the light beam of a photo cell
attached to the testing machine and sends a triggering signal to
the oscilloscope to start the sweep of the trace. A complete

28

description of the testing facility is given by Roberts and Krishna.[44]

The trace obtained on the oscilloscope was plotted on a Hewlett-Packard x-y recorder. A representative load-time trace is shown in Figure 8.

All low temperature specimens were cooled in a mechanically stirred 2-methylbutane bath cooled by liquid nitrogen. The specimens were held at temperature for a minimum of 15 minutes before testing and were tested within 20 seconds after removal from the bath.

All specimen dimensions were measured with a vernier caliper. The data was used to obtain the dynamic fracture toughness according to the theory outlined in the introduction.

RESULTS AND DISCUSSION

Hardness Tests

The hardness test results given in Figure 9 indicate that the weld metal is harder than the base plate and HAZ. The hardness levels of all three zones are not high. The absence of a highly hardened HAZ shows that no brittle martensite formed in the HAZ. This is not surprising since the carbon equivalent of A737 grade B is low. In addition, the welding parameters were selected for the purpose of suppressing the formation of martensite in the HAZ.

Tension Tests

The data obtained from the tension tests are presented in Table 2 and in Figures 10-12. The test results show that there is a decrease in yield strength and tensile strength of Armco W-19 weld metal with post-weld stress-relief heat treatment at 593°C. The drop in yield strength was not substantial, and even after 10 hours of post-weld stress relief, the weld metal still overmatched the base plate in yield and tensile strength. The room temperature yield strength of the weld metal declined from 511 MPa (74.1 Ksi) as welded to 480 MPa (69.6 Ksi) after 10 hours of post-weld heat treatment, while the room temperature tensile strength similarly dropped from 636 MPa (92.2 Ksi) to 573 MPa (83.0 Ksi). On the other hand, the elongation and reduction in area at room temperature increased with the post-weld heat treatment.

Figures 10 and 11 indicate that both the yield strength and tensile strength increase as the test temperature is lowered.

30

In the as welded condition, the yield strength increases from 511 MPa (74.1 Ksi) at room temperature to 574 MPa (83.2 Ksi) at -75°C (-103°F). The tensile strength increased in the same fashion from 636 MPa (92.2 Ksi) to 743 MPa (107.7 Ksi). However, the elongation and reduction in area did hot exhibit such a clear behavior.

Charpy Impact Tests

The Charpy impact test results are shown in Figures 13-18 and are summarized in Tables 3 and 4. The HAZ possessed a much higher upper shelf energy than the weld metal in all the heat treated conditions. However, the decline in toughness with a decrease in temperature was sharper in the HAZ than in the weld metal. While the 67.5 J (50 ft-lb) and 45 J (33 ft-lb) transition temperatures of the HAZ were lower than those of the weld metal, the opposite occurred with the 20 J (15 ft-lb) transition temperature.

The Charpy impact toughness of the weld metal and HAZ appeared to improve with post-weld heat treatment. After 10 hours of heat treatment, the transition temperatures for the weld were similar to those of the A737 B base plate. The HAZ exhibited lower toughness than the base plate in the as welded condition but was superior to the plate after 10 hours of post-weld heat treatment. The upper shelf energies of the HAZ and weld metal increased with the post-weld heat treatment. The toughness of the weldment in its entirety as determined by the Charpy impact tests was good.

NDTT Tests

The results of the Nil-Ductility Transition Temperature tests

31

performed on the weld metal are shown in Table 4. The NDTT was -95°C
(-139°F) for the as welded condition, -100°C (-148°F) for the 2 hour
stress relief condition, and -120°C (-184°F) for the 10 hour stress
relief condition. These values correlate well with the Charpy impact
test results. All three NDT temperatures are very close to the
corresponding 20 J (15 ft-lb) transition temperatures. Furthermore,
the increase in toughness produced by the post-weld stress relief
heat treatment is clearly indicated. Therefore, there is good
agreement between the Charpy impact tests and the NDTT tests.

Static Fracture Toughness Tests

The results acquired from the static fracture toughness tests
are given in Table 5 for the HAZ, and Table 6 for the weld metal.
The J-Δa curves obtained from the specimens tested at ambient
temperature are given in Figures 19-25. The J-Δa curve correspond-
ing to the base plate ambient temperature tests done by Qureshi[2],
is shown in Figure 20 for comparison. No J-Δa curves were plotted
for the tests performed at -50°C (-58°F) because no measurable crack
extension occurred before failure of the specimens.

The ambient temperature J_{1C} value of the base plate obtained
by Qureshi was 250 KJm^{-2} (119 ft-lb in.$^{-2}$). This value is larger
than those obtained for the HAZ. In the as welded condition, J_{1C}
was 185 KJm^{-2} (88 ft-lb in.$^{-2}$). After a 2 hour stress relief treat-
ment, J_{1C} was 161 KJm^{-2} (77 ft-lb in.$^{-2}$), and 173 KJm^{-2} (82 ft-lb
in.$^{-2}$) after a 10 hour stress relief treatment. Therefore, the post-
weld stress relief operation had little effect on the static fracture

toughness of the HAZ.

The toughness of the weld metal was noticeably lower than that of the HAZ in all three conditions of stress relief. J_{1C} was 123 KJm^{-2} (59 ft-lb in.$^{-2}$) in the as welded state, 121 KJm^{-2} (58 ft-lb in.$^{-2}$) after 2 hours of stress relief, and 118 KJm^{-2} (56 ft-lb in.$^{-2}$) after 10 hours of stress relief. Consequently, the effect of the post-weld stress relief heat treatment on the static fracture toughness of the weld metal was even smaller than the effect on the toughness of the HAZ.

The relative fracture toughness of the base plate, HAZ, and weld metal were in good agreement with the Charpy impact toughness of these three zones at 22°C. The base plate had an energy absorption of 210 J (155 ft-lb), the as welded HAZ around 170 J (125 ft-lb), and the weld metal about 130 J (96 ft-lb) at room temperature. This agreement does not hold for the HAZ and weld metal in the stress relieved condition. Although the energy absorption of the HAZ increased from 170 J to 224 J (165 ft-lb) after 10 hours of stress relief, the static fracture toughness dropped from 185 KJM^{-2} to 173 KJM^{-2}, a small decrease.

As discussed in the introduction, the J_{1C} value can, on certain occasions, be a very conservative value of fracture toughness, and a new parameter, called the Tearing Modulus, has been defined. This parameter has been calculated for all the material conditions tested at room temperature, and the results are given in Table 7. Since no J-Δa curves could be constructed for the specimens tested

at -50°C, no Tearing Modulus data was available at that temperature.

The Tearing Modulus of both the HAZ and weld metal increased with the post-weld stress relief heat treatment. The Tearing Modulus of the HAZ after a 10 hour stress relief treatment was higher than that of the base plate calculated from the test values reported by Qureshi.[2] The Tearing Modulus of the HAZ was considerably higher than that of the weld metal at all conditions of stress relief.

Therefore, the static fracture toughness data, interpreted using the Tearing Modulus parameter, would essentially agree with the findings of the Charpy impact tests in the sense that the post-weld stress relief heat treatment increased the toughness of the HAZ and the weld metal. However, as mentioned in the introduction, work is still necessary to fully understand the applicability of the Tearing Modulus parameter.

The temperature dependence of the static fracture toughness was clearly visible. The HAZ and weld metal experienced a decline in static fracture toughness with a decrease in temperature. The J_{1C} value of the as-welded HAZ dropped from 185 KJm^{-2} (88 ft-lb in.$^{-2}$) at 22°C (72°F) to 56 KJm^{-2} (27 ft-lb in.$^{-2}$). Similarly, the J_{1C} value of the weld metal dropped from 123 KJm^{-2} (59 ft-lb in.$^{-2}$) to 14 KJM^{-2} (7 ft-lb in.$^{-2}$) at -50°C.

The weld metal specimens tested at -50°C experienced a phenomenon known as "pop-in" during the static fracture toughness tests. This phenomenon can be described as a large and sudden

34

crack advance. When this occurred, a visible load drop was recorded on the load-face displacement trace. After "pop-in", the load rose to a maximum value where failure occurred. However, because of this "pop-in" phenomenon, failure conditions had to be calculated from the "pop-in" load and so, quite low fracture toughness values were obtained.

Dynamic Fracture Toughness Tests

The results of the dynamic fracture toughness tests conducted on the weld metal are given in Table 8. These results showed the same temperature dependance as the static fracture toughness results. The dynamic fracture toughness of the weld metal as welded dropped from 322 MPa m$^{\frac{1}{2}}$ (293 Ksi in$^{\frac{1}{2}}$) at room temperature to 132 MPa m$^{\frac{1}{2}}$ (120 Ksi in$^{\frac{1}{2}}$) at -50°C. The weld metal behaved similarly in the 2 hour stress relieved condition.

The weld metal dynamic fracture toughness was consistently higher than its static fracture toughness. This behavior is unusual but it has been reported before when the same testing method was used.[2,3] The problems inherent to this testing technique were already discussed in the introduction. In addition, the problem of load elevation due to the inertia of the test specimen was not entirely overcome although a cushion pad was used on each specimen. Therefore, the dynamic fracture toughness values measured can not be utilized in absolute terms and should only be used for comparison.

The room temperature dynamic fracture toughness of the metal declined after 2 hours of post-weld stress relief. However, the

decline was not very large. On the other hand, the dynamic
fracture toughness of the stress relieved weld metal at −50°C
was higher than that of the weld metal as welded.

Fracture Toughness Summary

The static fracture toughness data obtained from the J integral
tests are summarized in Table 9. The J_{1C} and $\bar{J}$ values measured
were converted to K using equation 13, because no valid K_{1C} by
ASTM specification E399 could be determined. Data obtained by
Qureshi[2] was also included for purposes of comparison. The results
indicated that the post-weld stress relief heat treatment had little
influence on the K values of the HAZ and weld metal. The HAZ and
weld metal exhibited lower toughness values than the base plate.
The weldment possessed high toughness at room temperature but the
toughness at −50°C (−58°F) was noticeably lower.

The crack toughness parameter proposed by Shoemaker and Rolfe[41]
was also calculated and included in Table 9. These ratios followed
the same trend established by the K values. The effect of the
stress relief treatment on the crack toughness parameter, as seen
in Table 9, was not significant.

CONCLUSIONS

As a result of the different mechanical tests performed on the A737 grade B weldment, the following was concluded:

1. The weld metal overmatched the strength of the base plate even after a 10 hour post-weld stress relief heat treatment at 593°C (1100°F). At room temperature, the yield strength of the weld metal as welded was 511 MPa (74.1 Ksi) compared to 389 MPa (56.4 Ksi) for the base plate, and the tensile strength was 636 MPa (92.2 Ksi) compared to 547 MPa (79.3 Ksi) for the base plate.

2. The base plate possessed a higher Charpy impact toughness than the HAZ which in turn was tougher than the weld metal. The upper shelf energy of the as welded HAZ was 168 J (124 ft-lb) compared to 133 J (98 ft-lb) of the weld metal. However, the decline in Charpy impact toughness with decreasing temperatures was sharper in the HAZ than in the weld metal.

3. In terms of Charpy impact transition temperature, the thermal stress relief operation proved beneficial for both the HAZ and weld metal. The 50 J (33 ft-lb) and 68 J (50 ft-lb) transition temperatures of the HAZ and weld metal were shifted 30°C (54°F) downwards after 10 hours of stress relief. The NDTT tests performed on the weld metal supported this conclusion.

4. The static fracture toughness of the HAZ, measured by J integral techniques, was superior at all heat treated conditions to the weld metal. The temperature dependence of fracture toughness was clearly visible. At -50°C, the HAZ had lost 45% of its toughness

37

at room temperature while the weld metal lost 60%.

    5.   The stress relief heat treatment had little effect on the static fracture toughness of the HAZ and weld metal. The fracture toughness (K) of the HAZ declined from 207 MPa $m^{\frac{1}{2}}$ (189 Ksi in.$^{\frac{1}{2}}$) to 200 MPa $m^{\frac{1}{2}}$ (182 Ksi in.$^{\frac{1}{2}}$) after 10 hours of stress relief. Likewise, the K value of the weld metal dropped from 169 MPa $m^{\frac{1}{2}}$ (154 Ksi in.$^{\frac{1}{2}}$) to 165 MPa $m^{\frac{1}{2}}$ (151 Ksi in.$^{\frac{1}{2}}$). The change in the dynamic fracture toughness of the weld metal followed the same pattern.

    6.   Although the fracture toughness of both the HAZ and weld metal decreased slightly after stress relief, the tearing modulus increased substantially. This seems to indicate that thermal stress relief provided the HAZ and weld metal with more ability to sustain stable crack growth.

Table 1. Summary of Material Specifications

A. Composition of A737 Grade B and ARMCO W-19 (wt%)

Identification	C	Mn	P	S	Si	Nb	Cu	Ni	Cr	Mo	Al
A737B Lukens Heat B1908 Analysis	.14	1.44	.009	.006	.19	.025	.27	.28	.22	.09	.030
ARMCO W-19 Specified Composition	.09	.85	.010	.008	.15	--	.25	3.5	.08	.03	--

B. Composition of Linde 709-5 Flux (%)

Identification	SiO_2	CaO	MnO	Al_2O_3	CaF_2
Linde 709-5	40	40	5	5	10

C. Transverse Tensile Properties of A737B (normalized)

Material	Yield MPa	Strength (ksi)	Tensile MPa	Strentgh (ksi)	Elongation %	R.A. %
A737B Heat B1908	389	(56.4)	547	(79.3)	29	58.1

Table 1. Continued

D. Charpy Impact Properties of A737B (normalized)

Material	Temperature °C (°F)		Energy Absorbed J (ft-lb)		Lateral Exp. mm (mils)		% Shear
A737B (normalized)	−46	(−50)	148	(109)	2.02	(80)	80
	−62	(−80)	145	(107)	2.01	(79)	80
	−73	(−100)	123	(91)	1.99	(78)	70

Table 2. Tension Test Date For A737 Grade B
Base Plate and ARMCO W-19 Weld Metal

Identification	Temperature °C	(°F)	Yield Strength MPa	(ksi)	Tensile Strength MPa	(ksi)	Elongation %	Red. in Area %
A737B *	22	(72)	366	(53.1)	513	(74.5)	36.5	-
Normalized	-46	(-50)	432	(62.7)	606	(88.0)	40.0	-
Transverse (TL)	-96	(-140)	506	(73.4)	693	(100.6)	40.8	-
ARMCO W-19	25	(77)	511	(74.1)	636	(92.2)	22.3	65.3
As Welded	-20	(-4)	536	(77.7)	667	(96.7)	24.8	67.1
Transverse	-50	(-58)	541	(78.4)	689	(99.9)	26.4	66.1
To Weld Direction	-75	(-103)	574	(83.3)	743	(107.7)	-	58.3
ARMCO W-19	25	(77)	514	(74.6)	614	(89.1)	25.3	66.0
Stress Relieved	-20	(-4)	526	(76.3)	636	(92.3)	24.8	66.2
2 Hours at 593°C	-50	(-58)	536	(77.8)	652	(94.6)	24.2	64.6
Transverse	-75	(-103)	567	(82.3)	683	(99.0)	25.9	64.9
ARMCO W-19	25	(77)	480	(69.6)	573	(83.0)	26.2	68.4
Stress Relieved	-20	(-4)	509	(73.7)	604	(87.6)	25.3	67.6
10 Hours at 593°C	-50	(-58)	523	(75.9)	630	(91.3)	27.9	65.2
Transverse	-75	(-103)	541	(78.5)	652	(94.5)	25.3	63.2

* From Reference 2

Table 3. Impact properties of A737 Grade B
Base Plate and Heat Affected Zone

Identification	Transition Temperatures Transverse (TL)							
	Impact Energy 20J (15 ft-1b)		Impact Energy 45J (33 ft-1b)		Impact Energy 68J (50 ft-1b)		Lateral Expansion .875mm (35 mil)	
	°C	(°F)	°C	(°F)	°C	(°F)	°C	(°F)
A737 Grade B*	-99	(-146)	-82	(-116)	-73	(-99)	-	-
A737 Grade B HAZ as welded	-90	(-130)	-72	(-98)	-62	(-80)	-72	(-98)
A737 Grade B HAZ stress relieved 2 hours	-115	(-175)	-100	(-148)	-92	(-134)	-92	(-134)
A737 Grade B HAZ stress relieved 10 hours	-115	(-175)	-105	(-157)	-94	(-137)	-95	(-139)

* From reference 2

Table 4. Impact Properties of ARMCO W-19 Weld Metal

A. Charpy Impact Test Results Transverse to Welding Direction

| Identification | Transition Temperature | | | | | | | |
| | Impact Energy 20J (15 ft-1b) | | Impact Energy 45J (33 ft-1b) | | Impact Energy 68J (50 ft-1b) | | Lateral Expansion .875mm (35 mil) | |
	°C	(°F)	°C	(°F)	°C	(°F)	°C	(°F)
ARMCO W-19 As welded	-96	(-141)	-56	(-69)	-30	(-22)	-43	(-45)
ARMCO W-19 Stress relieved 2 hours	-104	(-155)	-73	(-99)	-50	(-58)	-46	(-51)
ARMCO W-19 Stress relieved 10 hours	-113	(-171)	-86	(-123)	-62	(-80)	-58	(-72)

B. Drop Weight Test Results Transverse to Welding Direction

Identification	NDTT °C (°F)	Charpy Impact Energy at NDTT J (ft-1b)
ARMCO W-19 As welded	-95 (-139)	22 (16)
ARMCO W-19 Stress relieved 2 hours	-100 (-148)	23 (17)
ARMCO W-19 Stress relieved 10 hours	-120 (-184)	18 (13)

43

Table 5. Static Fracture Toughness of A737 Grade B HAZ

Identification	Specimen #	Test Temperature °C	(°F)	Crack Extension Δa mm	(in.)	J KJm^{-2}	(ft-lb in.$^{-2}$)
A737 Grade B	A72	22	(72)	.45	(.018)	217	(103)
	A71	22	(72)	.91	(.036)	374	(178)
HAZ As	A74	22	(72)	1.67	(.066)	380	(181)
	A73	22	(72)	2.01	(.079)	589	(280)
					J_{IC} =	185	(88)
Welded	A105	−50	(−58)	−	−	32	(15)
	A106	−50	(−58)	.33	(.013)	73	(35)
Transverse (TL)	A107	−50	(−58)	.12	(.005)	84	(40)
	A108	−50	(−58)	−	−	36	(17)
					$\overline{J}$ =	56	(27)
A737 Grade B	A85	22	(72)	.27	(.011)	182	(87)
	A92	22	(72)	.58	(.023)	232	(110)
	A91	22	(72)	.87	(.034)	289	(137)
HAZ Stress R.	A93	22	(72)	1.09	(.043)	336	(160)
					J_{IC} =	161	(77)
2 hours at 593°C	A86	−50	(−58)	−	−	38	(18)
	A87	−50	(−58)	−	−	72	(35)
Transverse (TL)	A88	−50	(−58)	−	−	42	(20)
					$\overline{J}$ =	51	(24)

Table 5. Continued

	Specimen #	Test Temperature °C	(°F)	Crack Extension Δa mm	(in.)	J KJm^{-2}	(ft-lb in.$^{-2}$)
A737 Grade B	A131	22	(72)	.40	(.016)	233	(111)
HAZ Stress R.	A133	22	(72)	.46	(.018)	297	(141)
10 hours at 593°C	A132	22	(72)	.65	(.025)	353	(168)
Transverse (TL)	A134	22	(72)	.86	(.034)	423	(201)
				J_{IC} =		173	(82)

Table 6. Static Fracture Toughness of ARMCO W-19 Weld Metal

Identification	Specimen #	Test Temperature °C	(°F)	Crack Extension mm	(in.)	J_{IC} KJm^{-2}	(ft-lb in.$^{-2}$)
ARMCO W-19 As Welded Transverse to Welding direction	A103	22	(72)	.40	(.016)	140	(67)
	A102	22	(72)	.92	(.036)	177	(84)
	A101	22	(72)	1.06	(.042)	187	(89)
	A104	22	(72)	1.86	(.073)	234	(112)
				J_{IC} =		123	(59)
	A76	-50	(-58)	*		17	(8)
	A77	-50	(-58)	*		12	(6)
	A78	-50	(-58)	*		15	(7)
				$\overline{J}$ =		14	(7)
ARMCO W-19 Stress R. 2 hours at 593°C Transverse to welding direction	A82	22	(72)	.38	(.015)	131	(62)
	A83	22	(72)	.44	(.017)	143	(68)
	A84	22	(72)	.66	(.026)	154	(73)
	A98	22	(72)	.72	(.028)	182	(87)
	A81	22	(72)	1.39	(.055)	204	(97)
				J_{IC} =		121	(58)
	A95	-50	(-58)	*		20	(9)
	A96	-50	(-58)	*		16	(8)
	A97	-50	(-58)	*		20	(9)
				$\overline{J}$ =		19	(9)

Table 6. Continued

	Specimen #	Test Temperature °C	(°F)	Crack Extension mm	(in.)	J KJm^{-2}	(ft-lb in.$^{-2}$)
ARMCO W-19	A135	22	(72)	.31	(.012)	130	(62)
Stress R.	A138	22	(72)	.40	(.016)	185	(88)
10 hours at 593°C	A136	22	(72)	.70	(.027)	214	(102)
Transverse to	A137	22	(72)	.96	(.038)	247	(117)
welding direction				J_{IC} =		118	(56)

47

* "pop-in"

Table 7. Tearing Modulus Data for A737 Grade B
Base Plate and HAZ, and ARMCO W-19 Weld Metal

Identification	Test Temperature °C	(°F)	dJ/da KJm^{-2}/mm	Tearing Modulus T=(dJ/da)(E/σo^2)
A737 Grade B Base Plate *	23	(73)	327.63	358.6
A737 Grade B HAZ As welded	22	(72)	192.24	173.7
A737 Grade B HAZ Stress R. 2 hours at 593°C	22	(72)	214.86	212.4
A737 Grade B HAZ Stress R. 10 hours at 593°C	22	(72)	380.28	379.6
ARMCO W-19 As welded	22	(72)	64.42	41.3
ARMCO W-19 Stress R. 2 hours at 593°C	22	(72)	68.82	45.6
ARMOC W-19 Stress R. 10 hours at 593°C	22	(72)	157.13	119.5

* Obtained from data in reference 2

48

Table 8. Dynamic Fracture Toughness Data for ARMCO W-19 Weld Metal

A. Weld Metal As Received Transverse to Welding Direction

Specimen #	Test Temperature °C	(°F)	W_m J	(ft-lb)	JC_d KJm^{-2}	(ft-lb $in.^{-2}$)	K_{dt} $MPa\ m^{\frac{1}{2}}$	($ksi\ in.^{\frac{1}{2}}$)
A151	22	(72)	88.2	(65.0)	467	(222)	329	(299)
A152	22	(72)	83.6	(61.6)	428	(204)	315	(287)
Average			85.9	(63.3)	448.5	(213)	322	(293)
A153	-50	(-58)	14.8	(10.9)	73	(35)	130	(118)
A154	-50	(-58)	14.9	(11.0)	78	(37)	134	(122)
Average			14.85	(10.95)	75.5	(36)	132	(120)

B. Weld Metal Stress Releived 2 Hours at 593°C Transverse to Welding Direction

Specimen #	Test Temperature °C	(°F)	W_m J	(ft-lb)	JC_d KJm^{-2}	(ft-lb $in.^{-2}$)	K_{dt} $MPa\ m^{\frac{1}{2}}$	($ksi\ in.^{\frac{1}{2}}$)
A155	22	(72)	69.1	(50.9)	362	(172)	289	(263)
A156	22	(72)	61.9	(45.7)	323	(154)	274	(249)
Average			65.5	(48.3)	342.5	(163)	281.5	(256)
A157	-50	(-58)	18.1	(13.4)	93	(44)	147	(134)
A158	-50	(-58)	15.7	(11.6)	80	(38)	136	(124)
Average			16.9	(12.5)	86.5	(41)	141.5	(129)

49

Table 9. Static Fracture Toughness Summary

Identification	Test Temperature °C	(°F)	KJ MPa $m^{\frac{1}{2}}$	(ksi in.$^{\frac{1}{2}}$)	KJ/σ_{ys} $m^{\frac{1}{2}}$	(in.$^{\frac{1}{2}}$)
A737 Grade B	23	(73)	241 *	(219)	.658	(4.13)
Base Plate	-4	(-4)	234 *	(213)	.539	(3.38)
(from reference 2)	-96	(-141)	147 **	(134)	.292	(1.83)
A737 B HAZ	22	(72)	207 *	(189)	.514	(3.23)
As Welded	-50	(-58)	114 **	(104)	.264	(1.66)
A737B HAZ	22	(72)	193 *	(176)	.504	(3.16)
Stress R. 2 hours	-50	(-58)	109 **	(99)	.263	(1.65)
A737B HAZ Stress R. 10 hours	22	(72)	200 *	(182)	.524	(3.29)
ARMCO W-19	22	(72)	169 *	(154)	.330	(2.07)
As Welded	-50	(-58)	57 **	(52)	.112	(.70)
ARMCO W-19	22	(72)	167 *	(152)	.326	(2.05)
Stress R. 2 hours	-50	(-58)	66 **	(60)	.128	(.80)
ARMCO W-19 Stress R. 10 hours	22	(72)	165 *	(151)	.345	(2.16)

* K_{IC} calculated from J_{IC} ($K_{IC} = \sqrt{J_{IC}} \sqrt{E/1-\nu^2}$)

** K calculated from $\overline{J}$ (K = $\sqrt{J}$ $\sqrt{E/1-\nu^2}$)

102 mm

26mm

52 mm

51
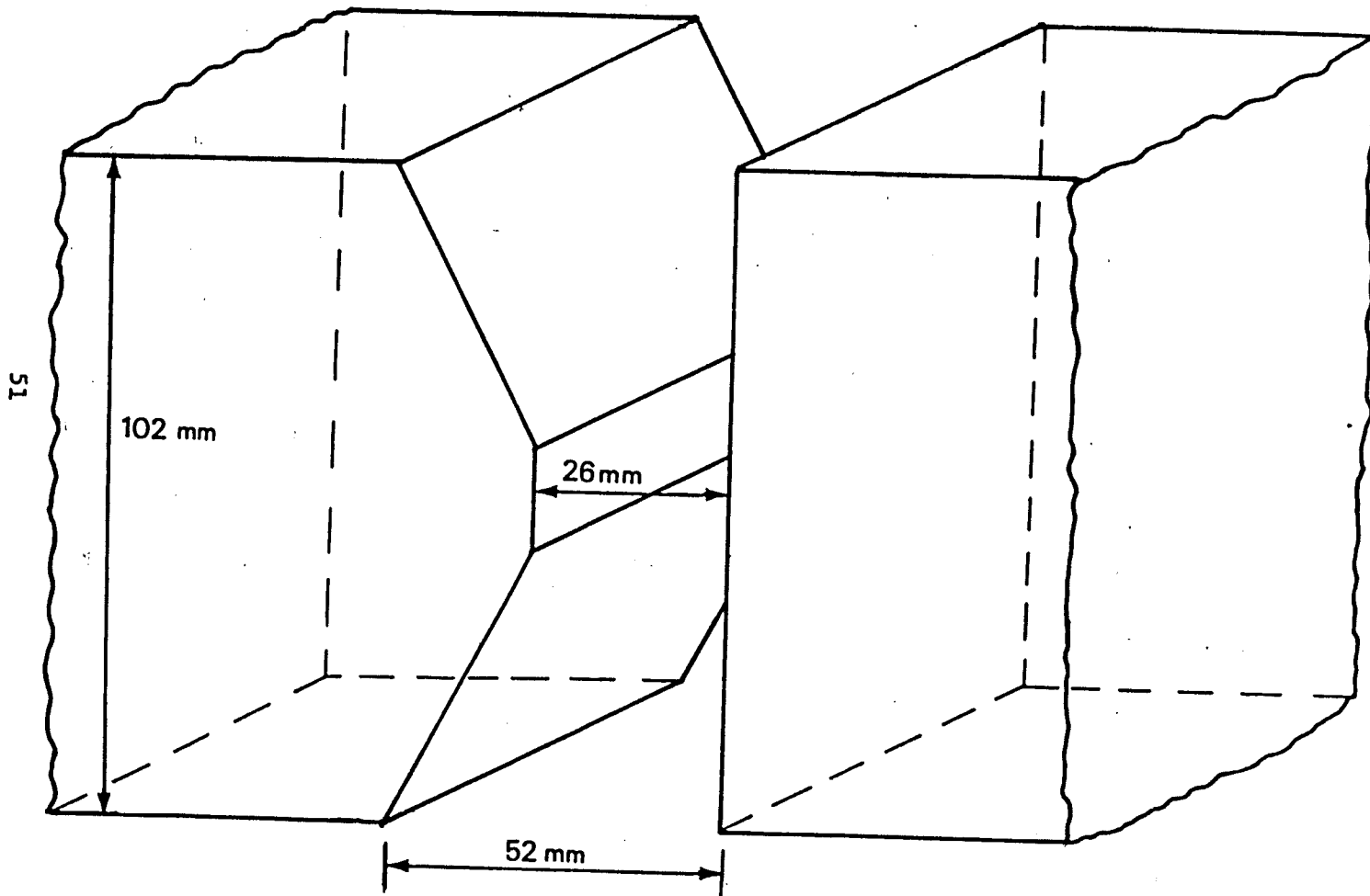
FIGURE 1.   "K" WELD GROOVE
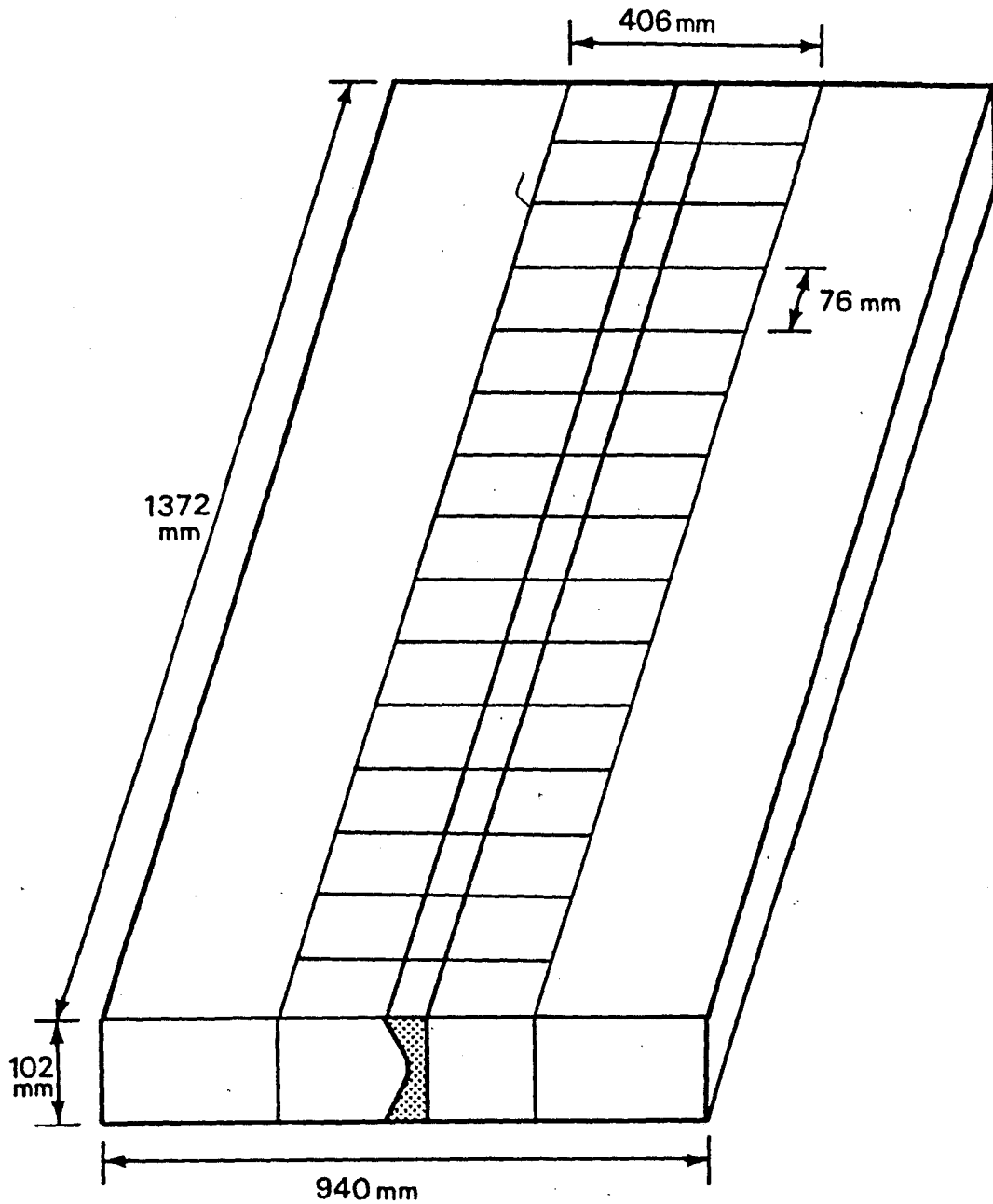
FIGURE 2. SECTIONING DIAGRAM OF WELDED PLATE

52
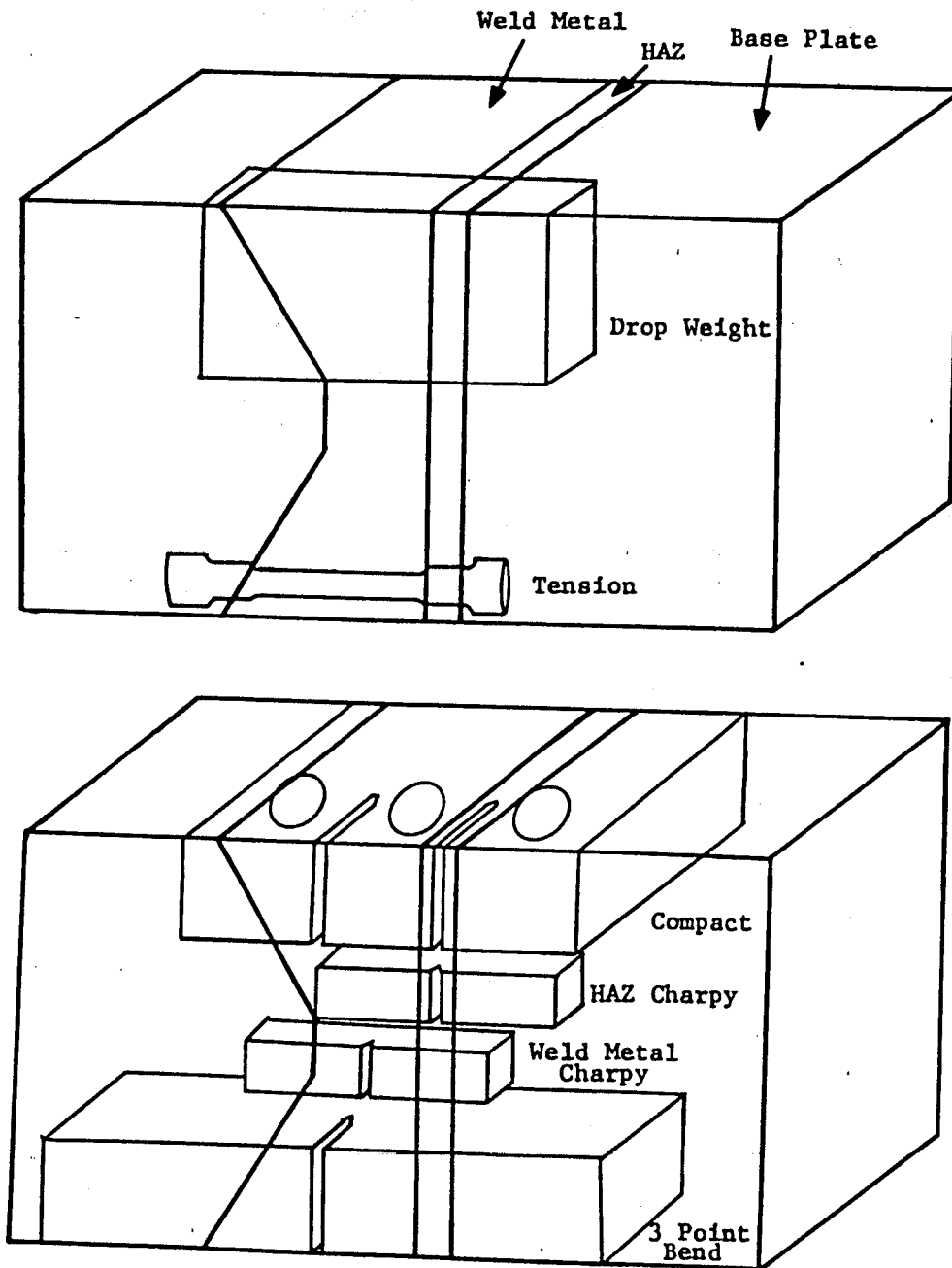
FIGURE 3.   SPECIMEN LAYOUT

53

50 ±1mm

16 ± .5mm

54

130 ±10 mm
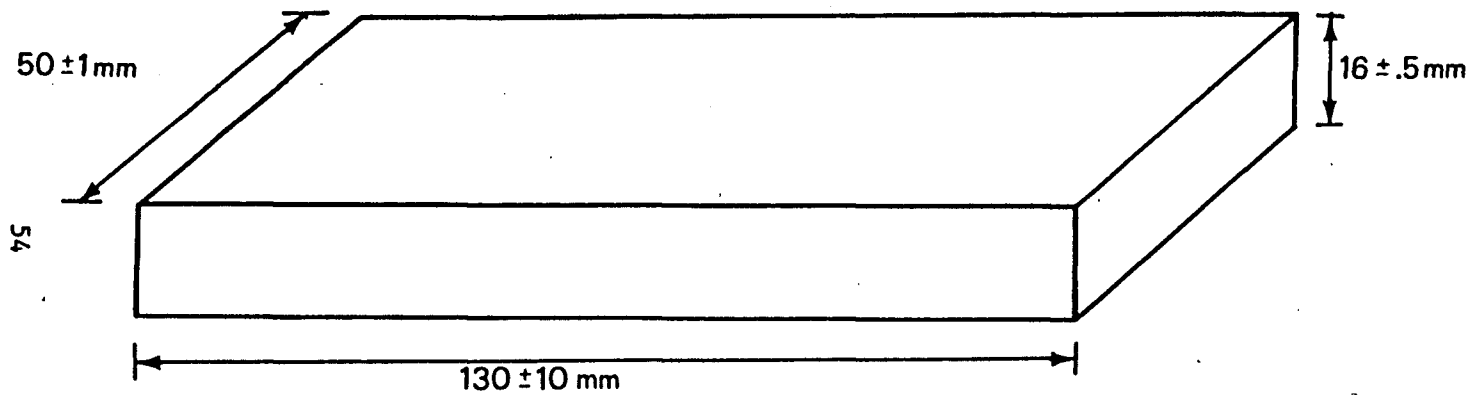
FIGURE 4.   DROP WEIGHT SPECIMEN
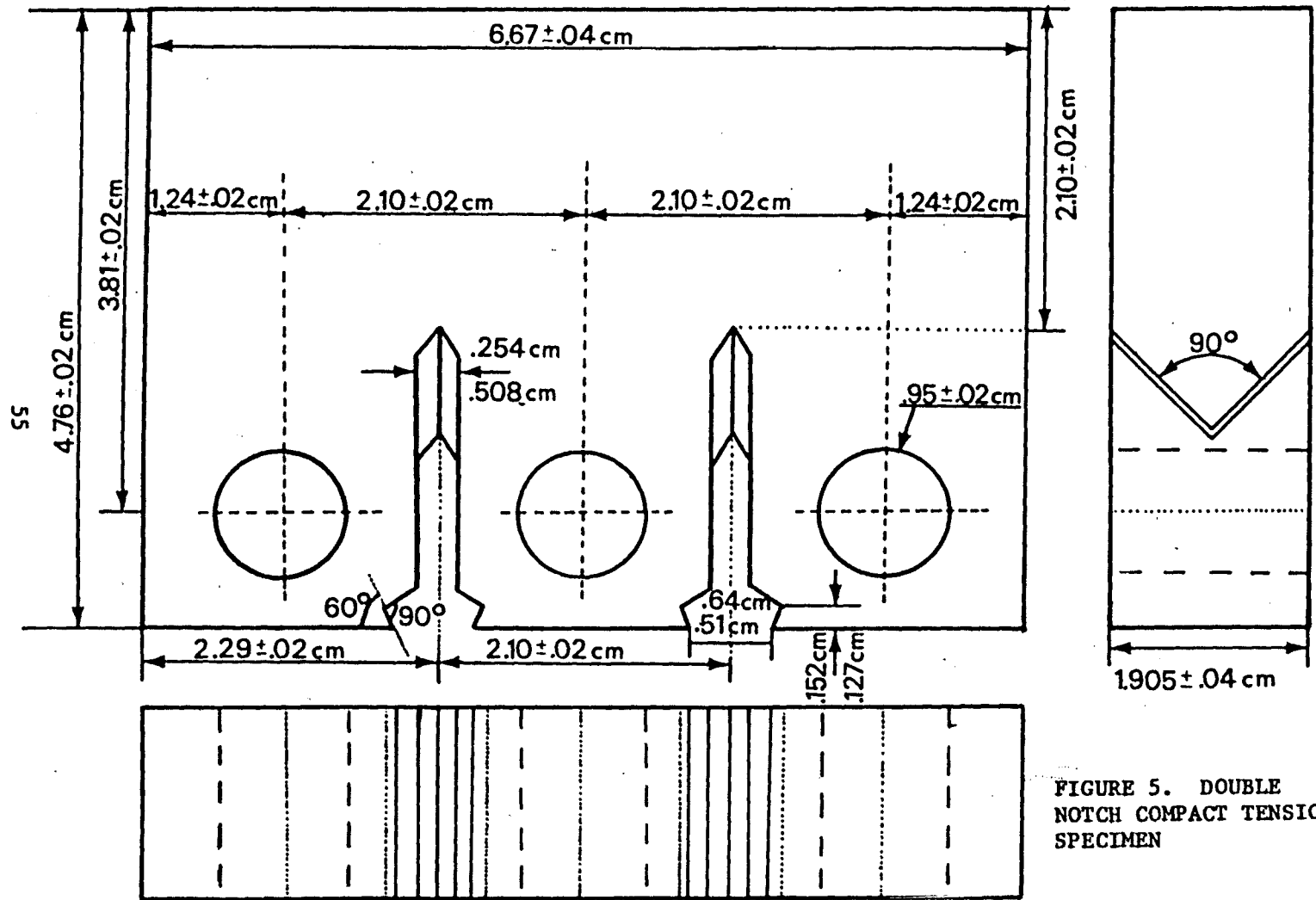
FIGURE 5. DOUBLE NOTCH COMPACT TENSION SPECIMEN

Dimensions shown: 6.67±.04 cm, 2.10±.02 cm, 3.81±.02 cm, 4.76±.02 cm, 1.24±.02 cm, 2.10±.02 cm, 2.10±.02 cm, 1.24±.02 cm, .254 cm, .508 cm, .95±.02 cm, 60°, 90°, 2.29±.02 cm, 2.10±.02 cm, .64 cm, .51 cm, .152 cm, .127 cm, 1.905±.04 cm, 90°

55
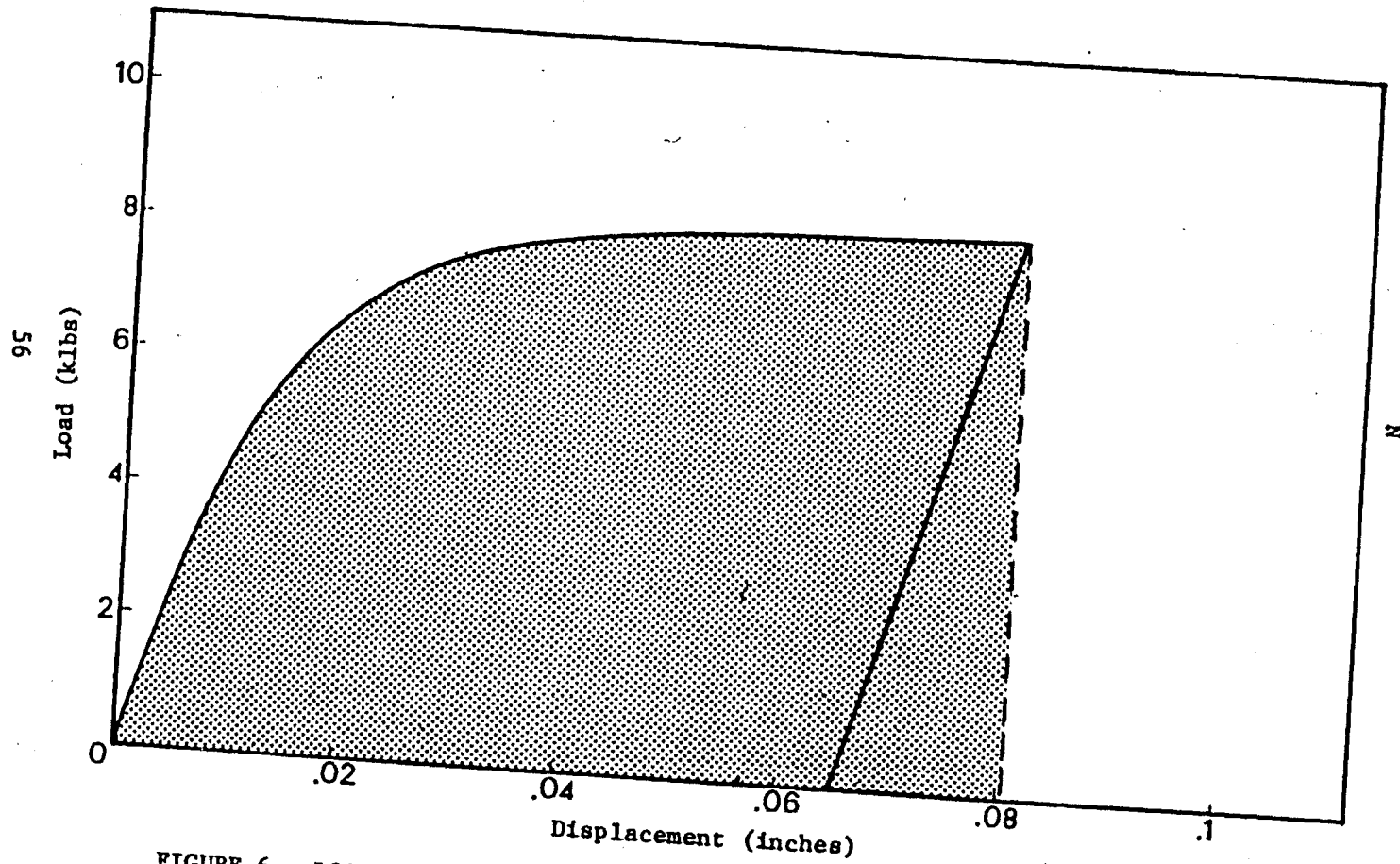
FIGURE 6.   LOAD-FACE DISPLACEMENT TRACE FOR STATIC FRACTURE TOUGHNESS TEST

56
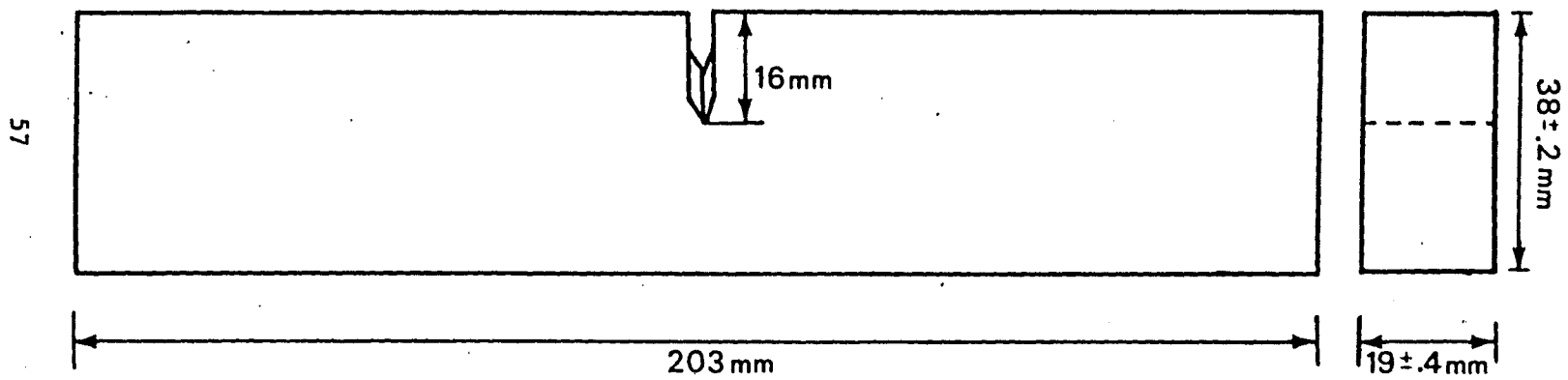
FIGURE 7. THREE POINT BEND SPECIMEN
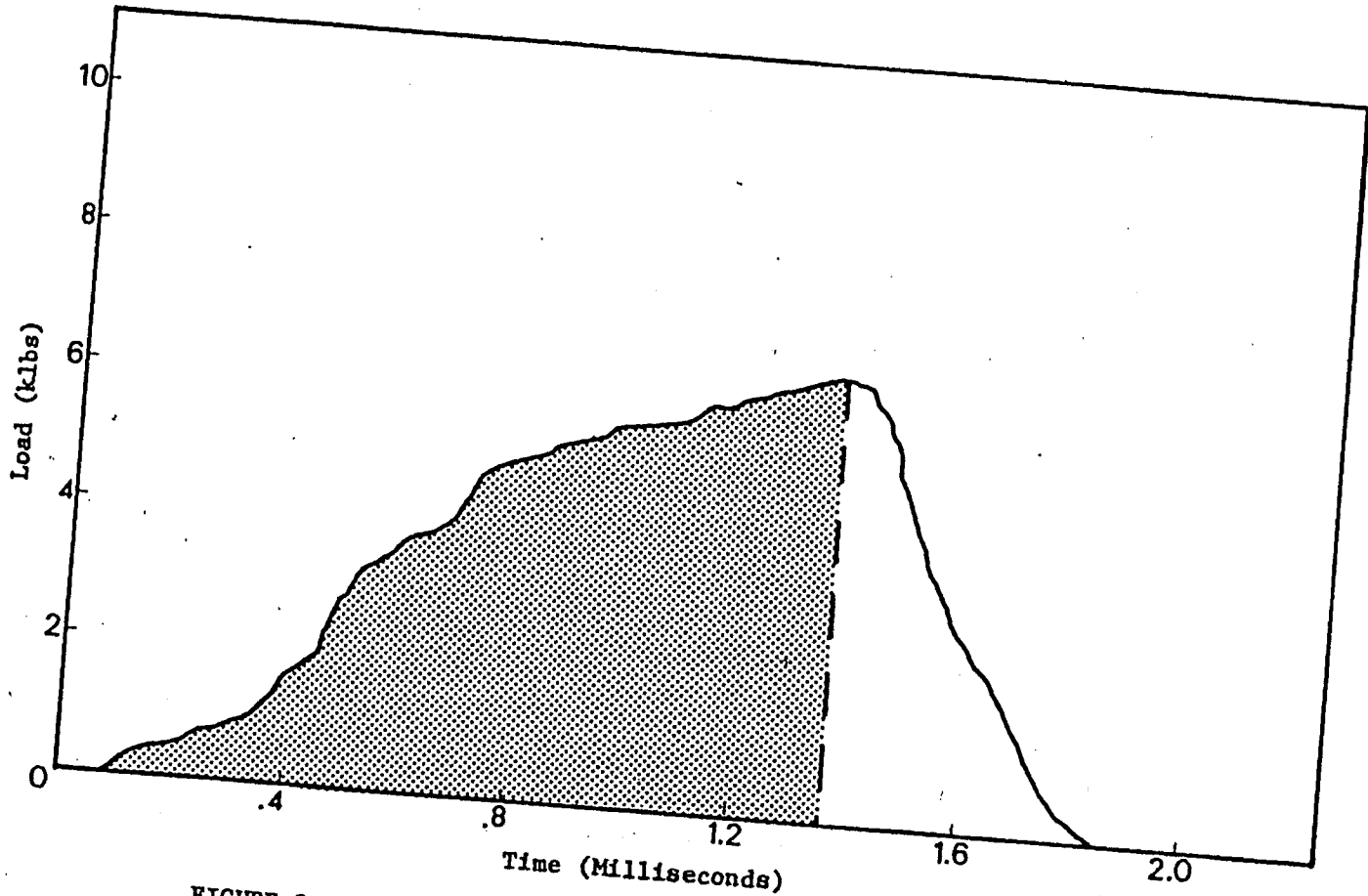
FIGURE 8. LOAD-TIME TRACE FOR DYNAMIC FRACTURE TOUGHNESS TEST
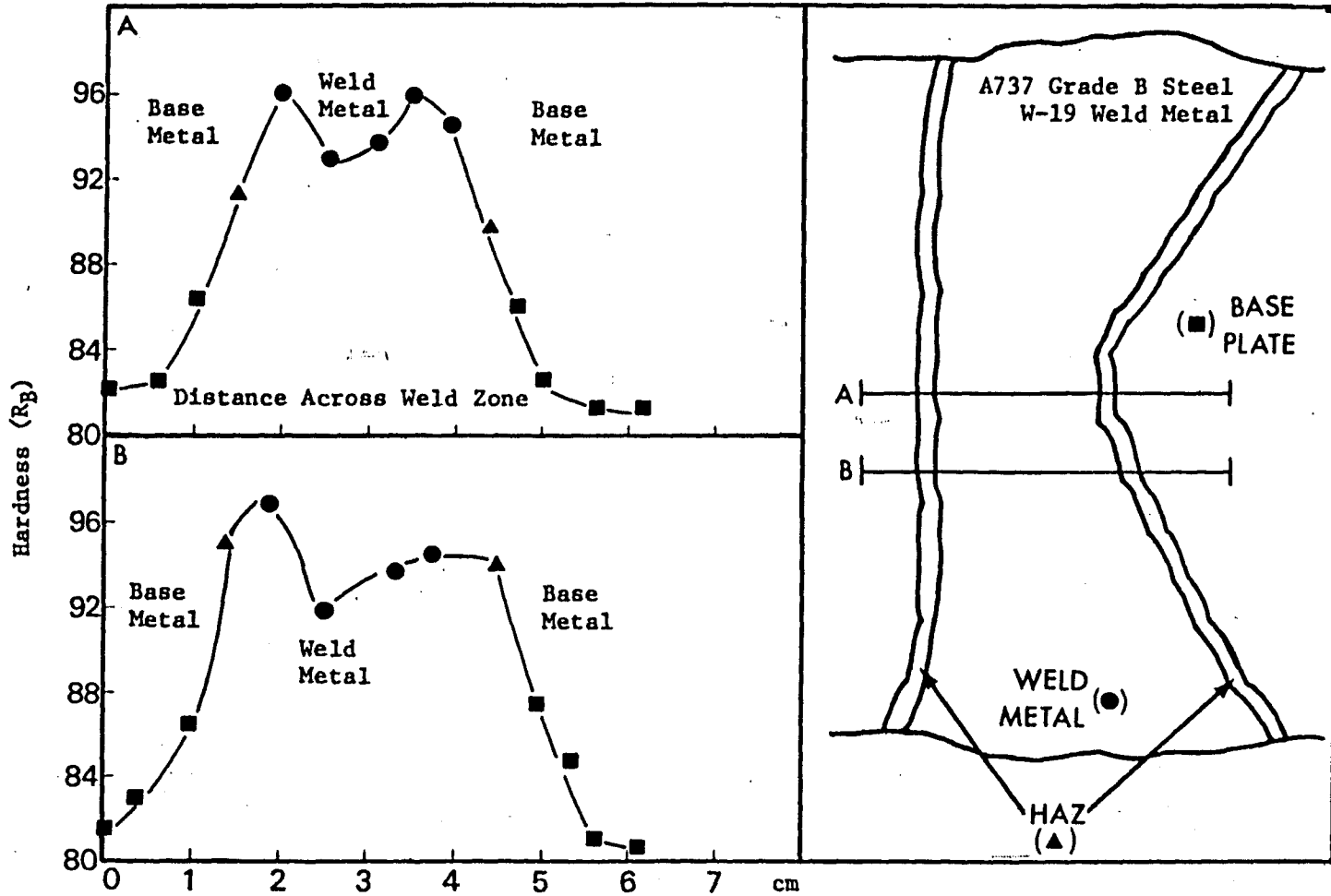
FIGURE 9.   HARDNESS TRAVERSE ACROSS A737B WELD
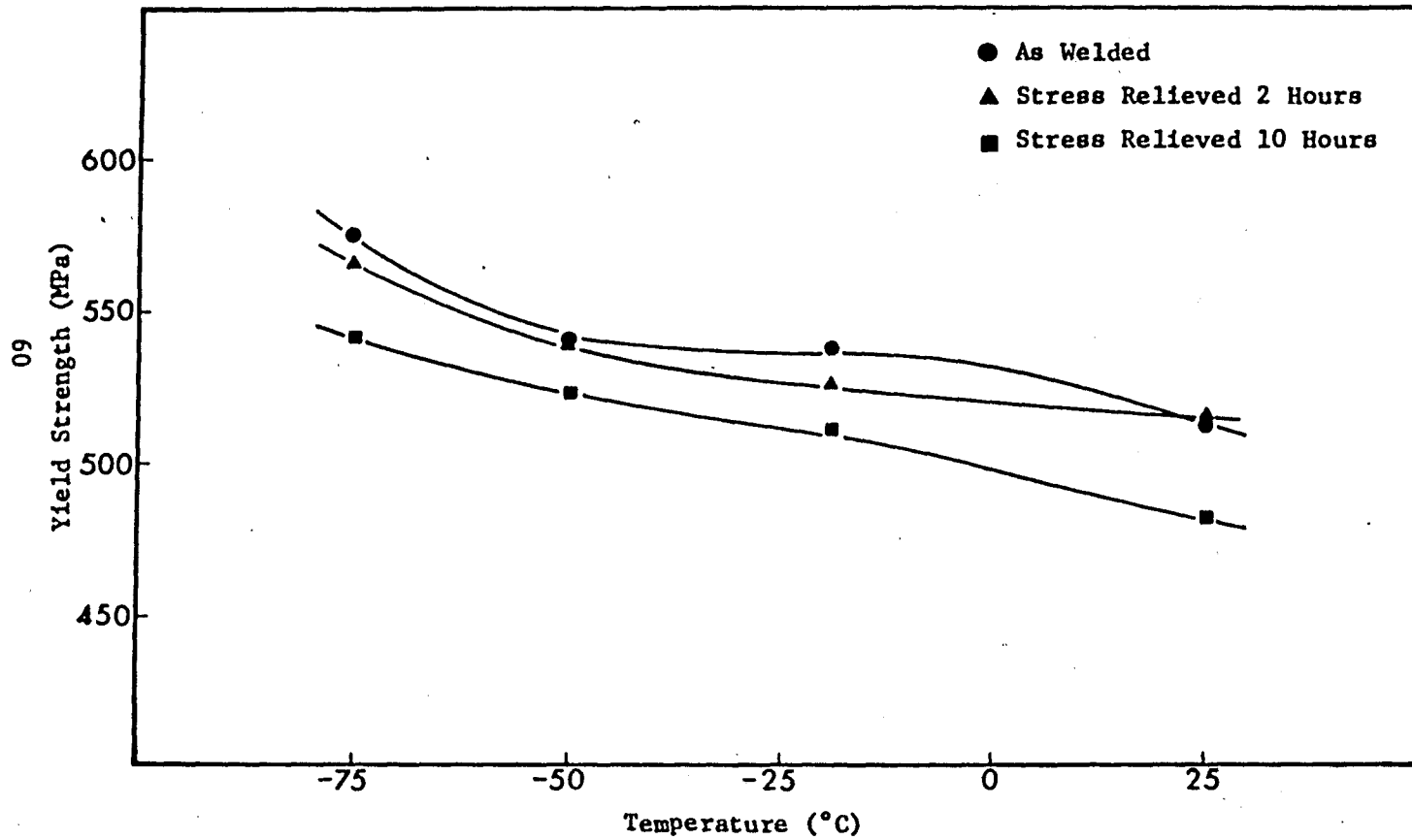
FIGURE 10.   YIELD STRENGTH VS. TEMPERATURE ARMCO W-19 WELD METAL
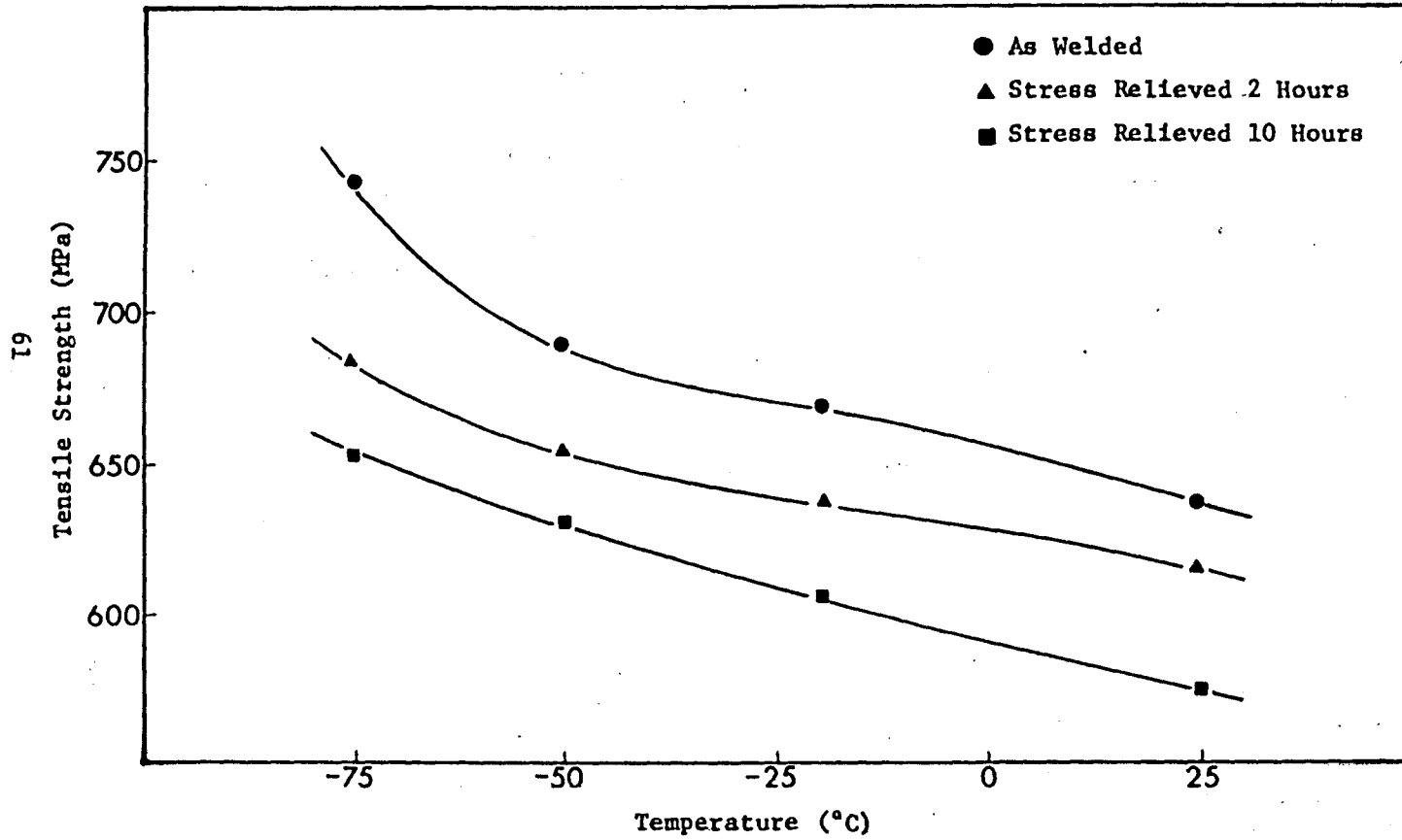
FIGURE 11.   TENSILE STRENGTH VS. TEMPERATURE ARMCO W-19 WELD METAL
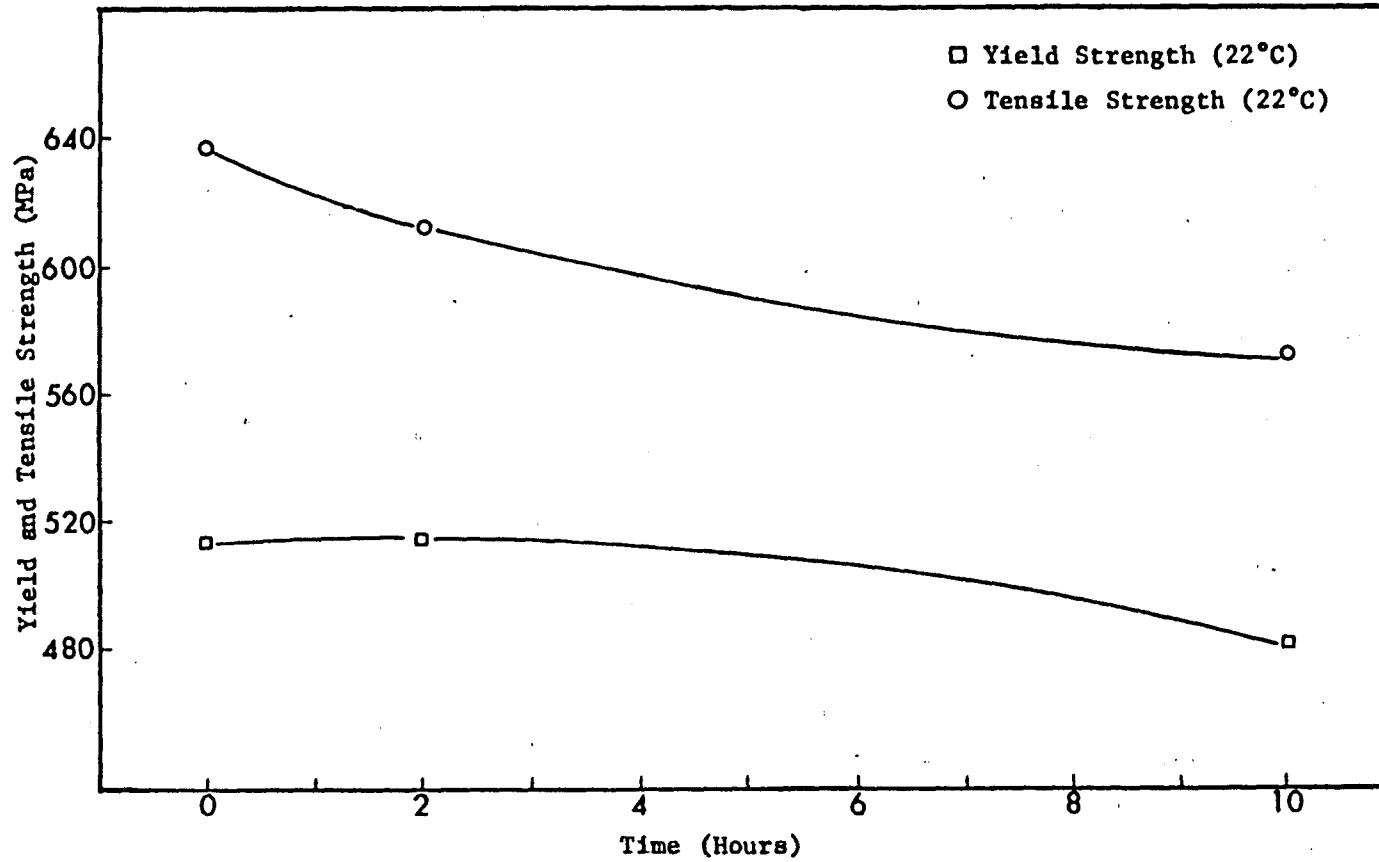
FIGURE 12.   YIELD STRENGTH AND TENSILE STRENGTH OF ARMCO W-19 VS. STRESS RELIEF TIME
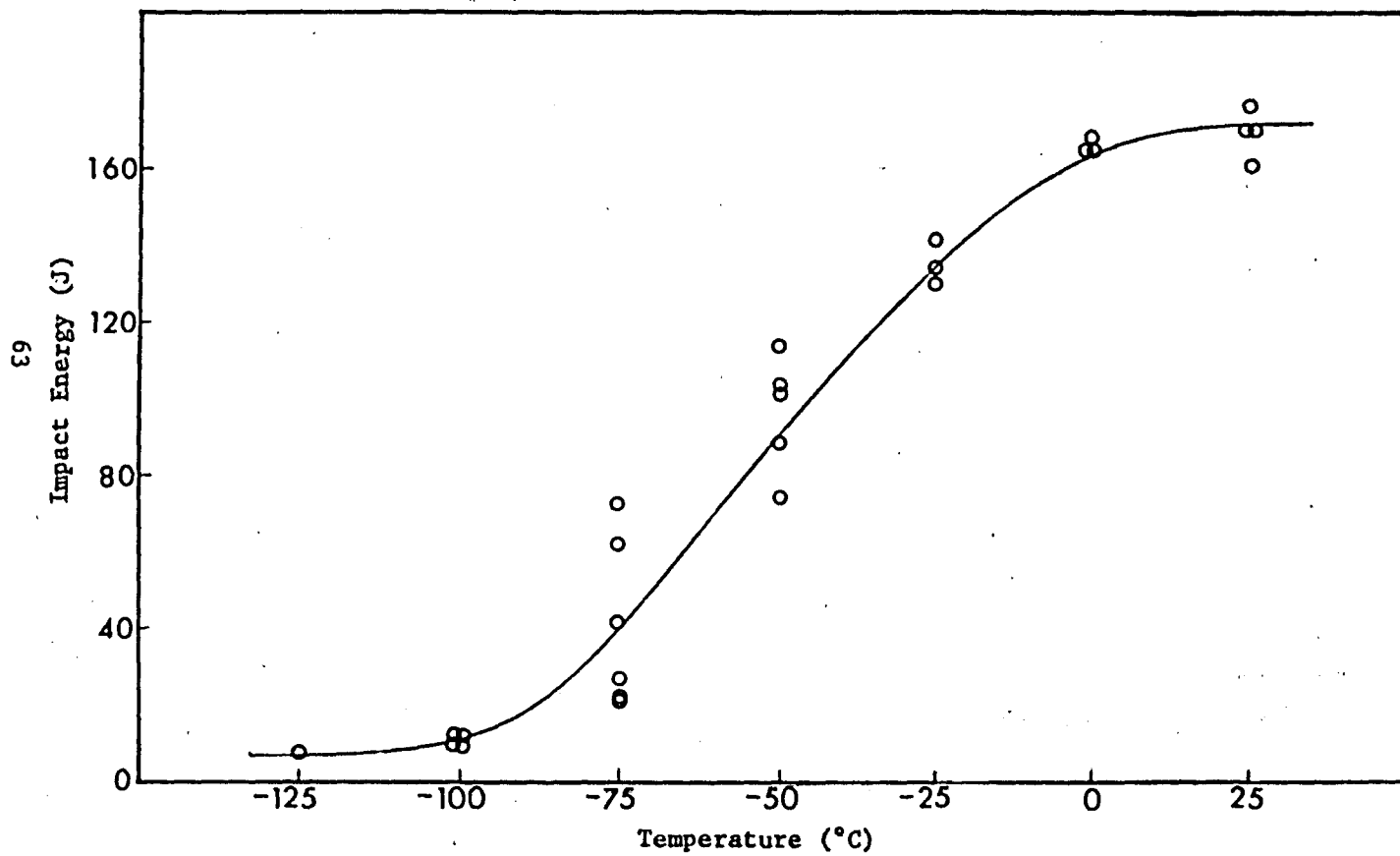
FIGURE 13A.   CHARPY IMPACT ENERGY VS. TEMPERATURE A737B HAZ AS WELDED

63
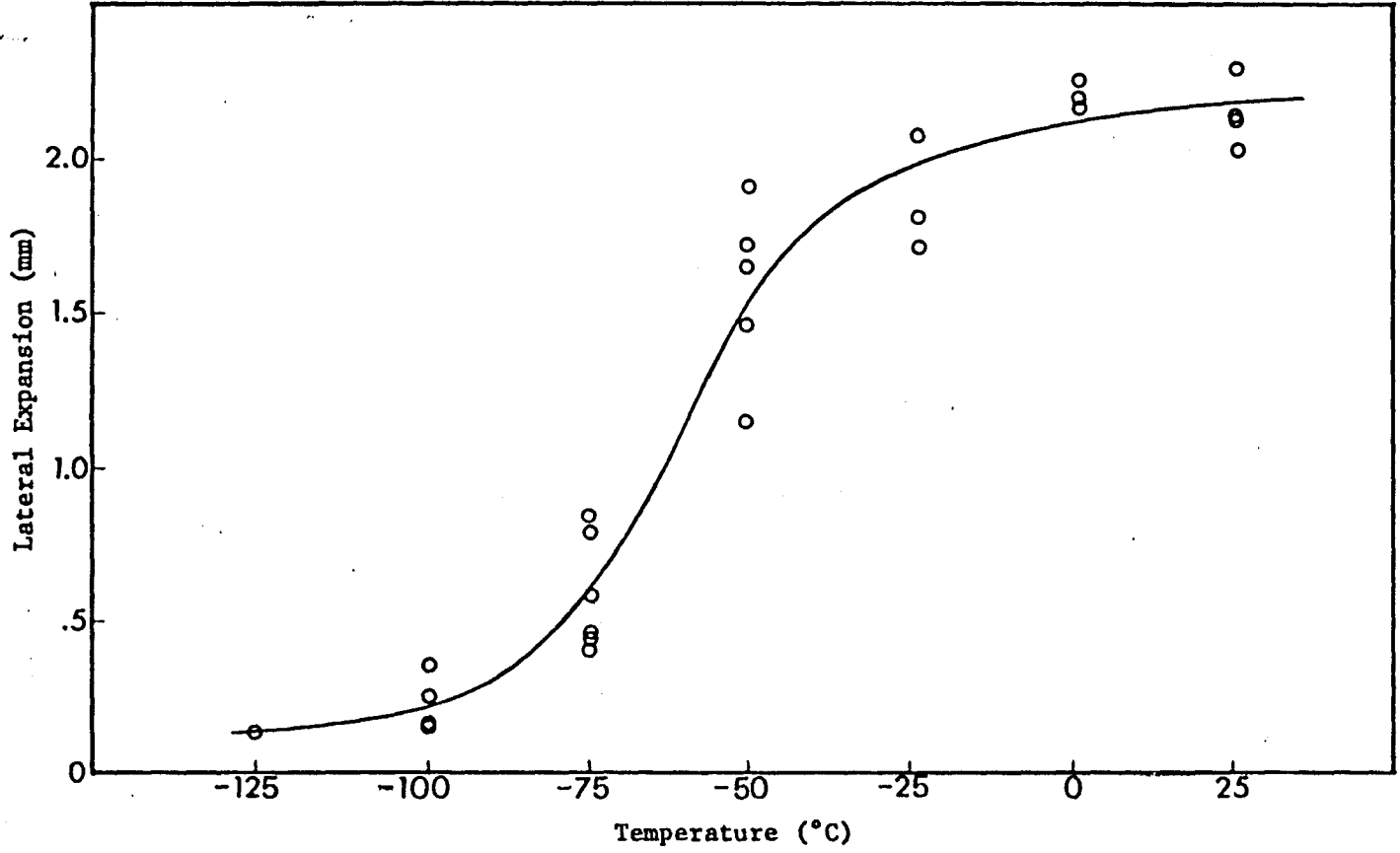
FIGURE 13B.   CHARPY LATERAL EXPANSION VS. TEMPERATURE A737B HAZ AS WELDED
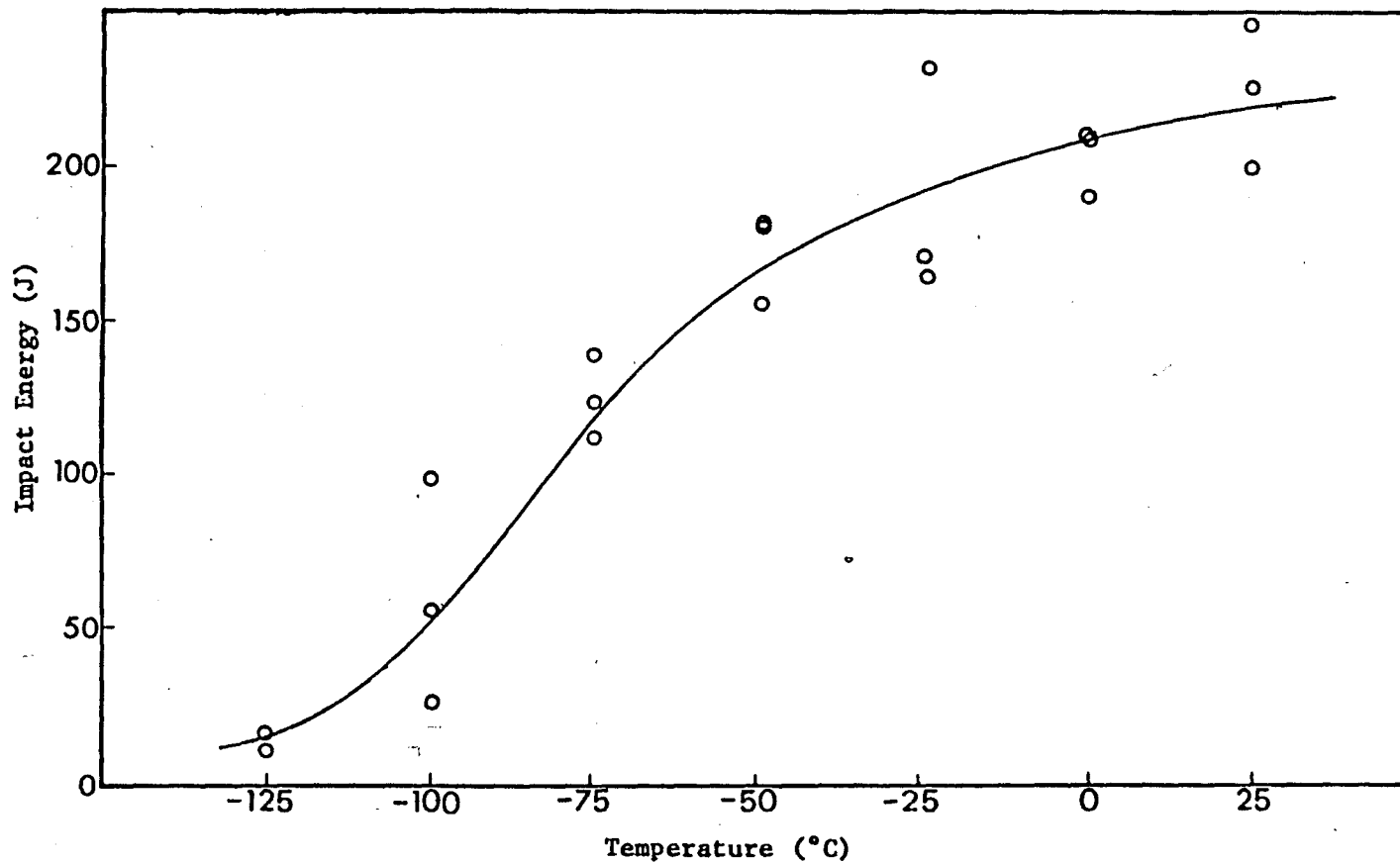
FIGURE 14A.   CHARPY IMPACT ENERGY VS. TEMPERATURE A737B HAZ STRESS RELIEVED 2 HOURS
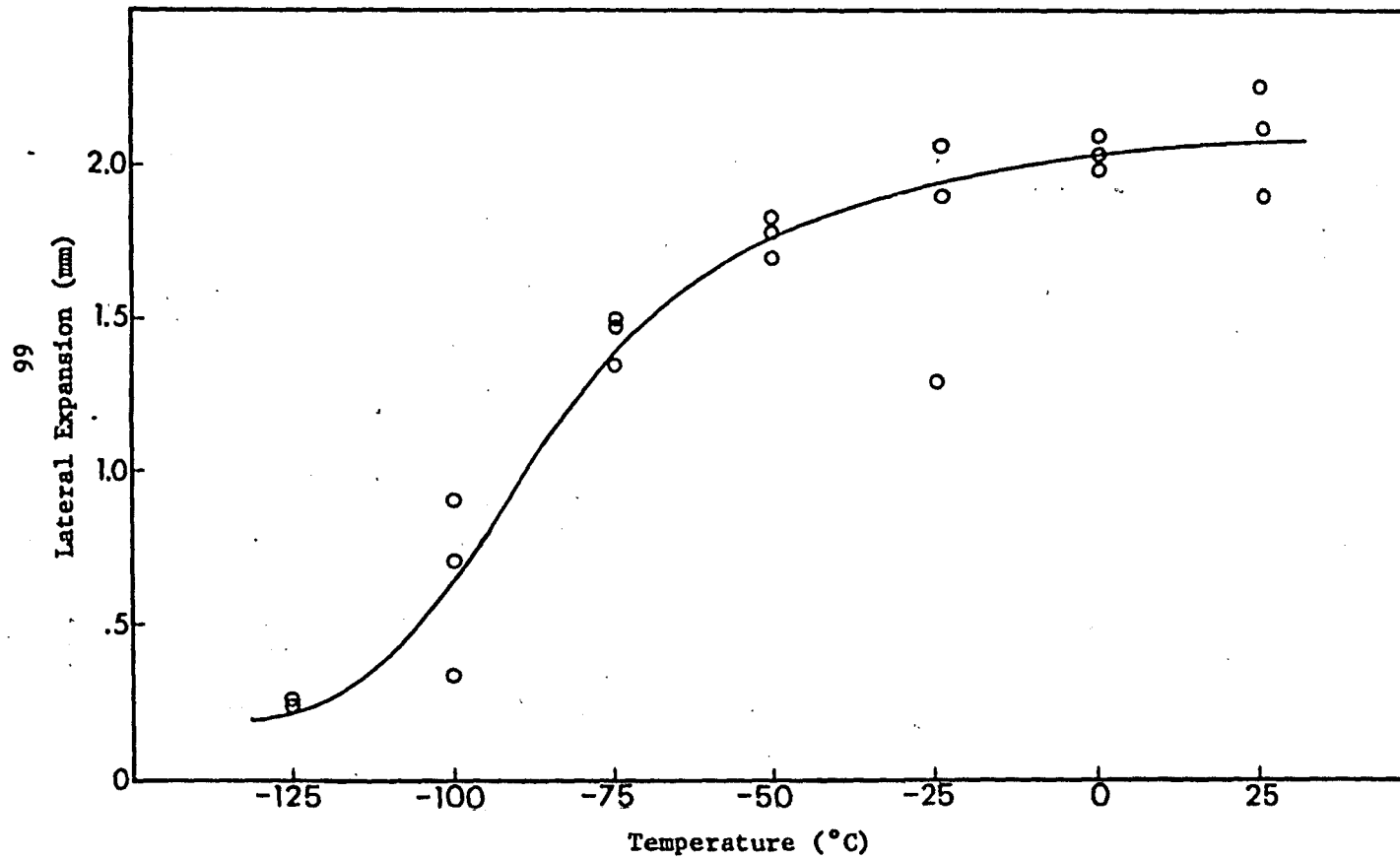
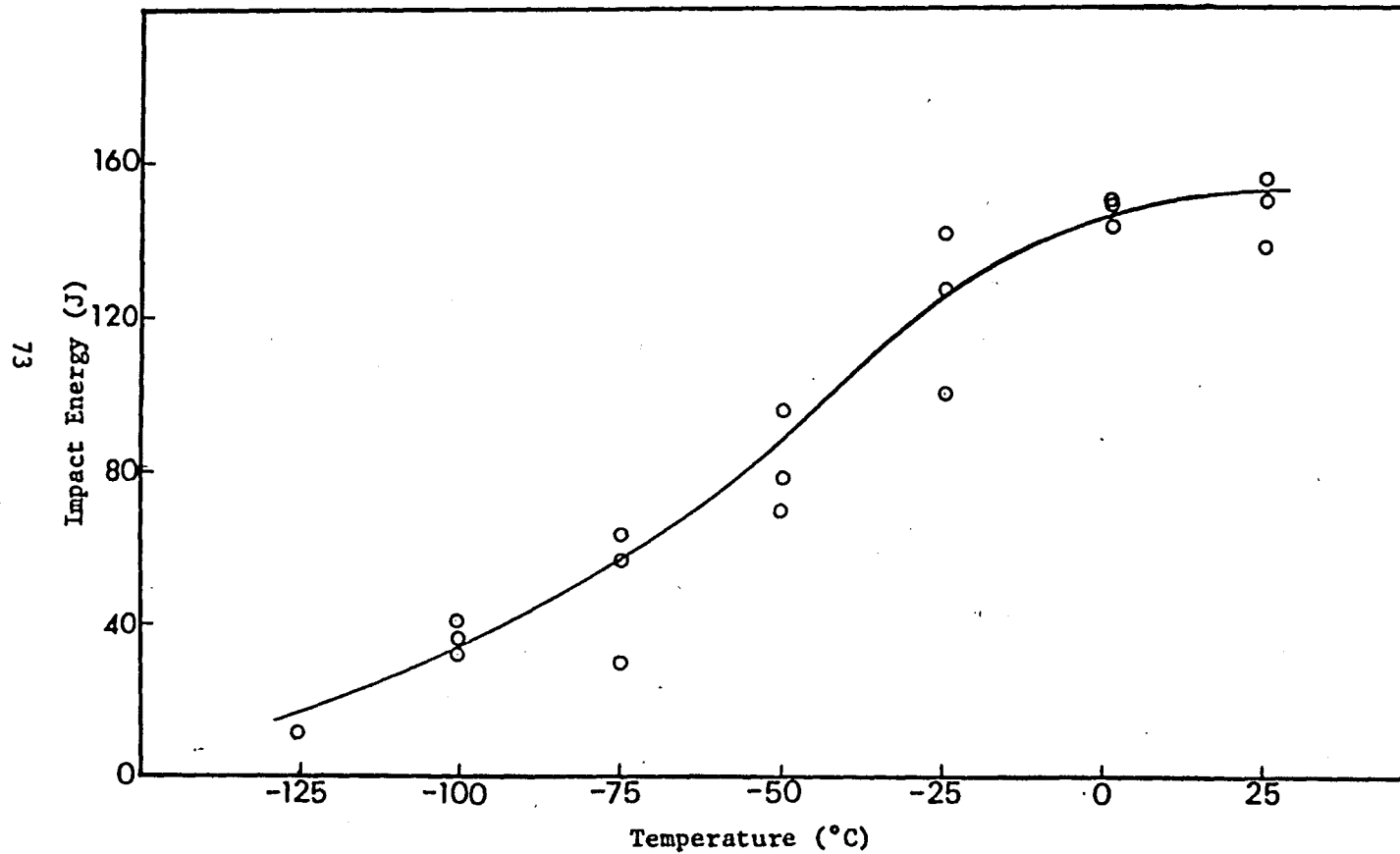FIGURE 14B.   CHARPY LATERAL EXPANSION VS. TEMPERATURE A737B HAZ STRESS RELIEVED 2 HOURS
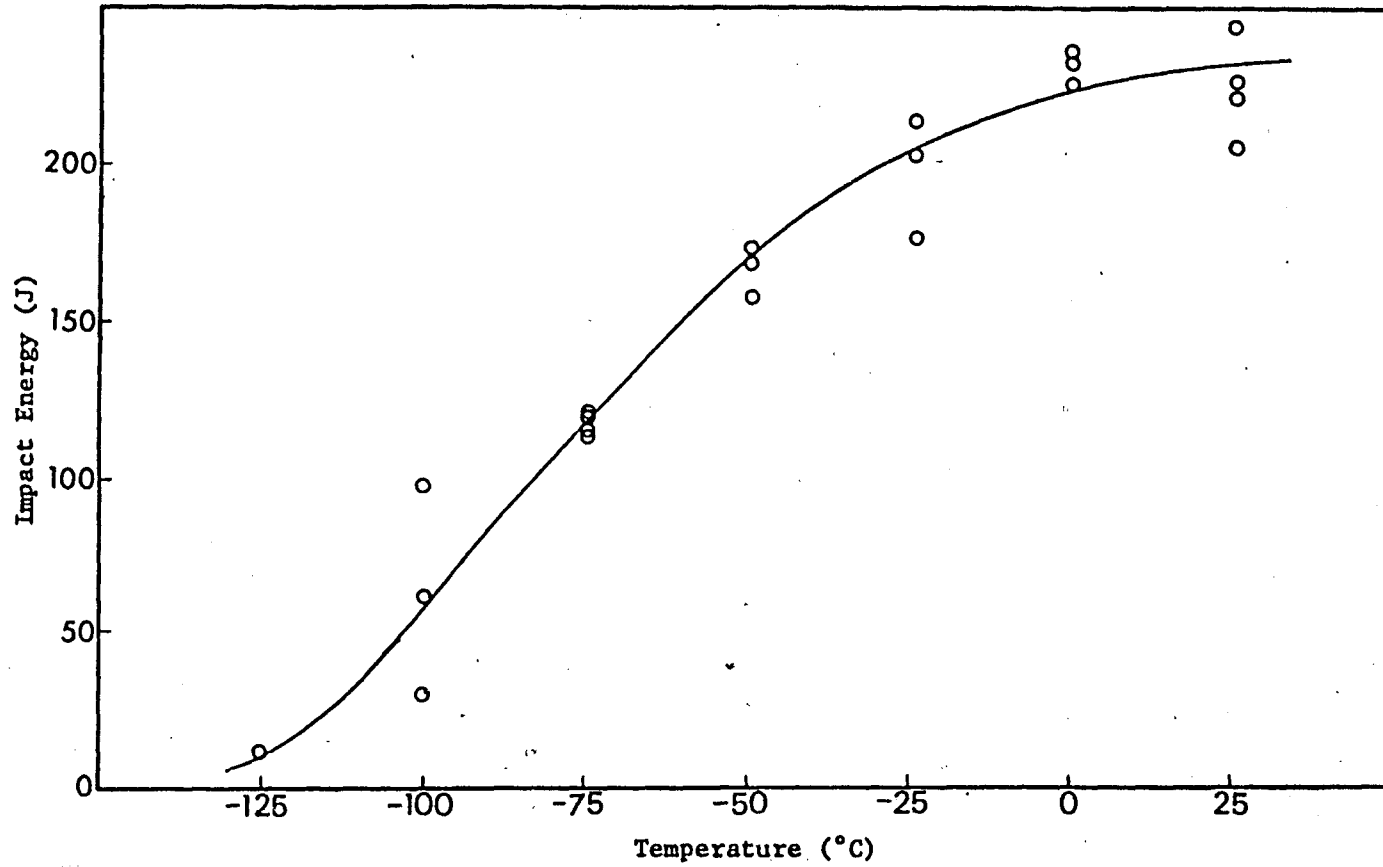
FIGURE 15A.   CHARPY IMPACT ENERGY VS. TEMPERATURE A737B HAZ STRESS RELIEVED 10 HOURS
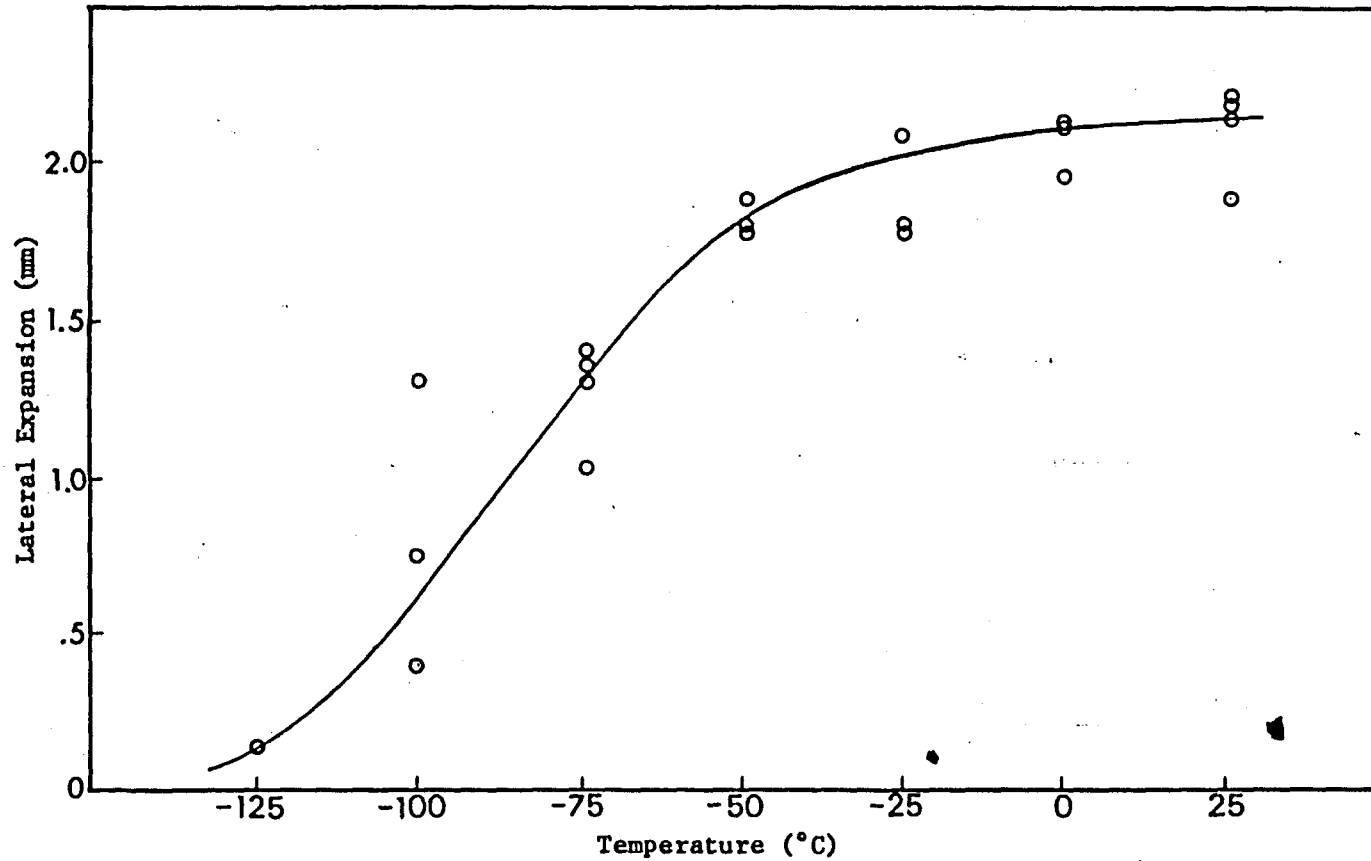
FIGURE 15B.   CHARPY LATERAL EXPANSION VS. TEMPERATURE A737B HAZ STRESS RELIEFED 10 HOURS
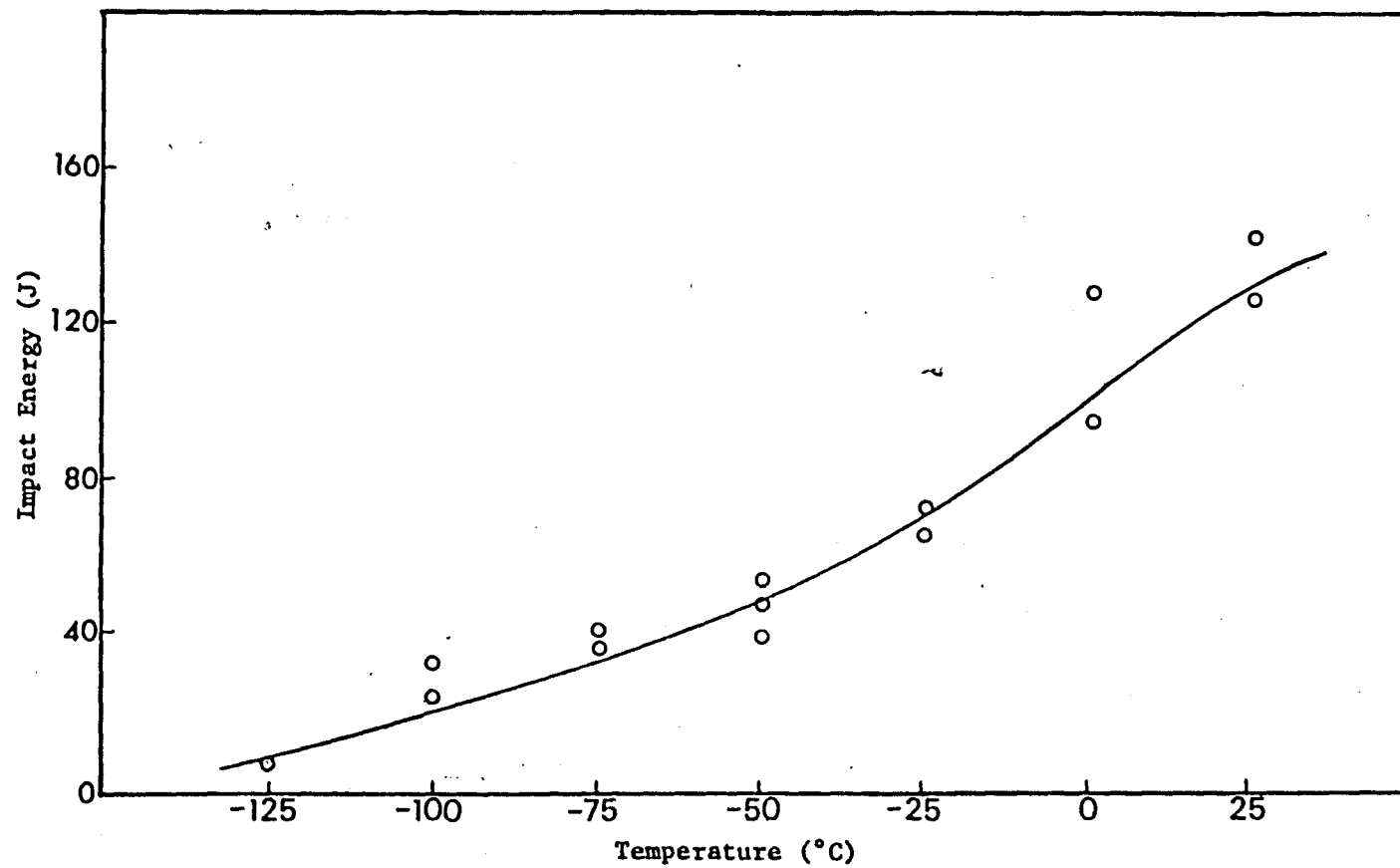
FIGURE 16A.   CHARPY IMPACT ENERGY VS. TEMPERATURE ARMCO W-19 WELD METAL AS WELDED

FIGURE 16B.   CHARPY LATERAL EXPANSION VS. TEMPERATURE ARMCO W-19 WELD METAL AS WELDED

70
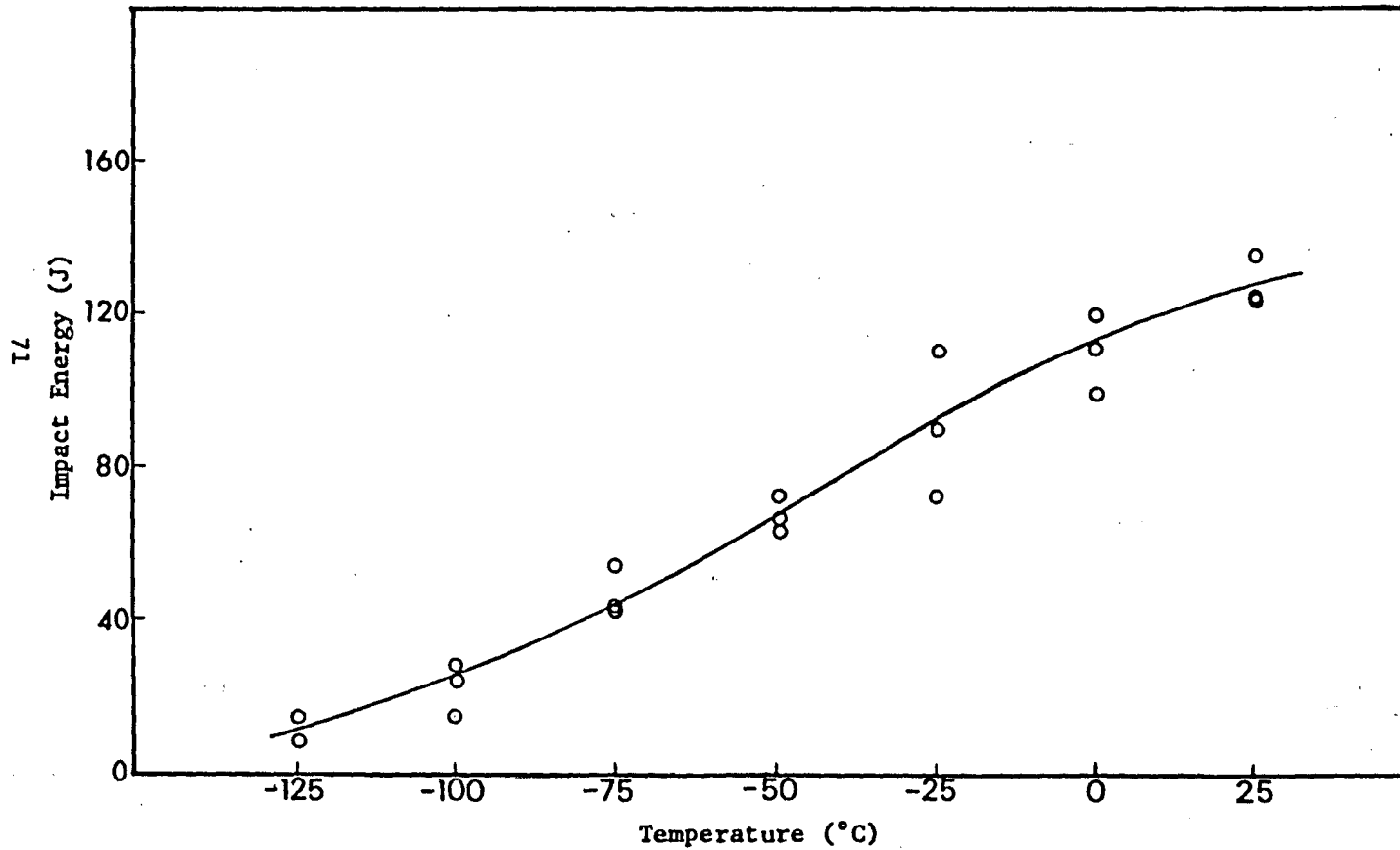
FIGURE 17A. CHARPY IMPACT ENERGY VS. TEMPERATURE ARMCO W-19 WELD METAL STRESS RELIEVED 2 HOURS
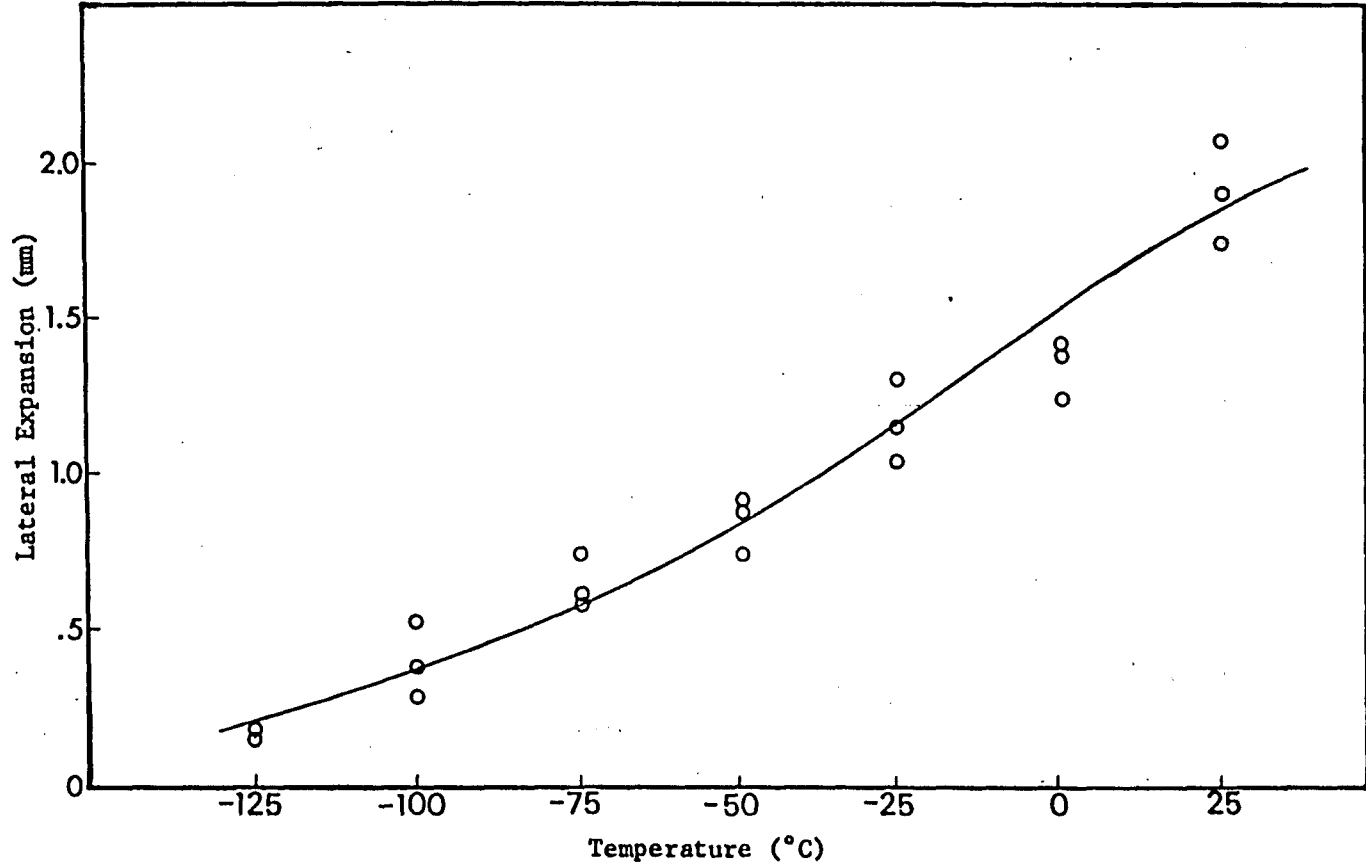
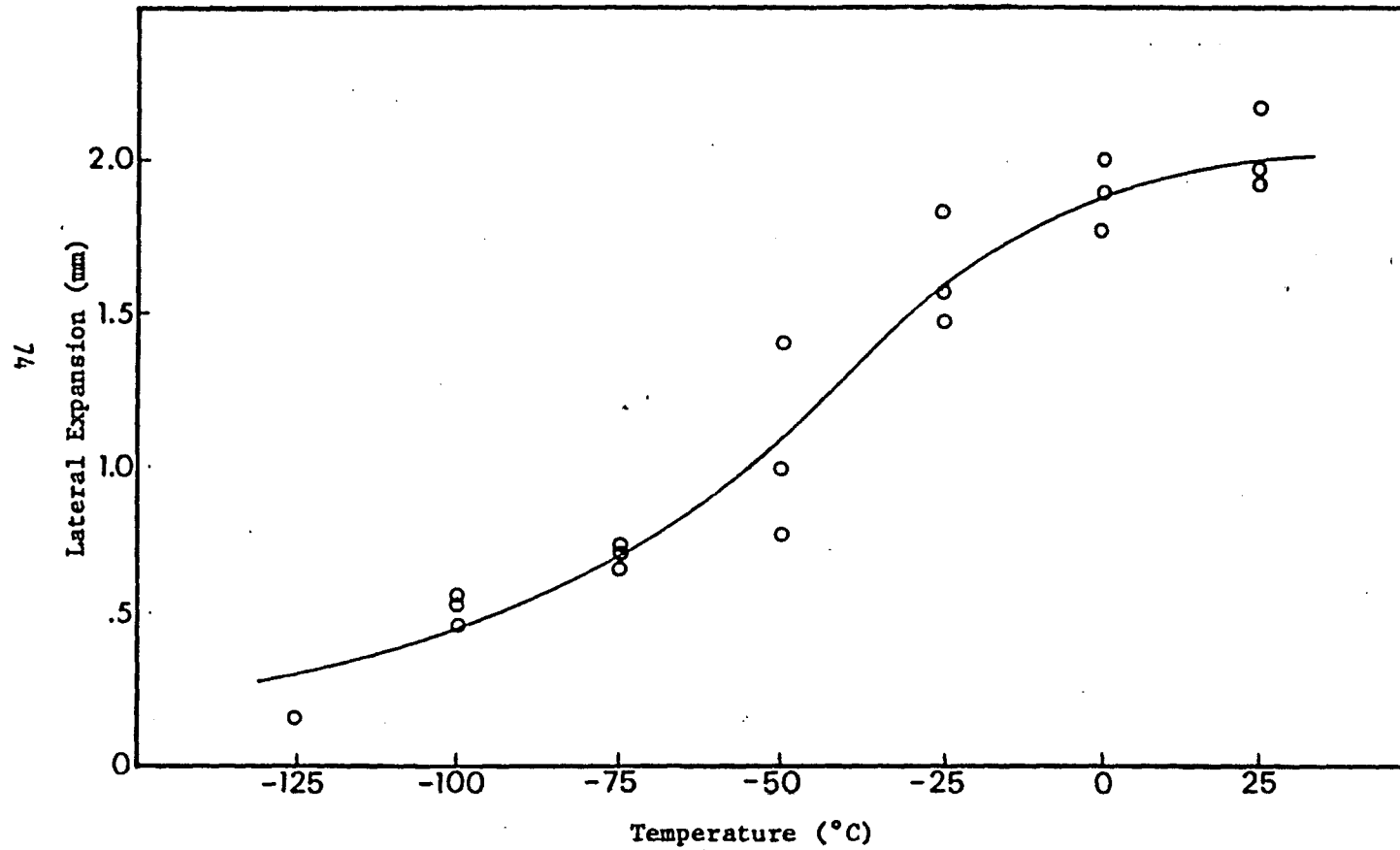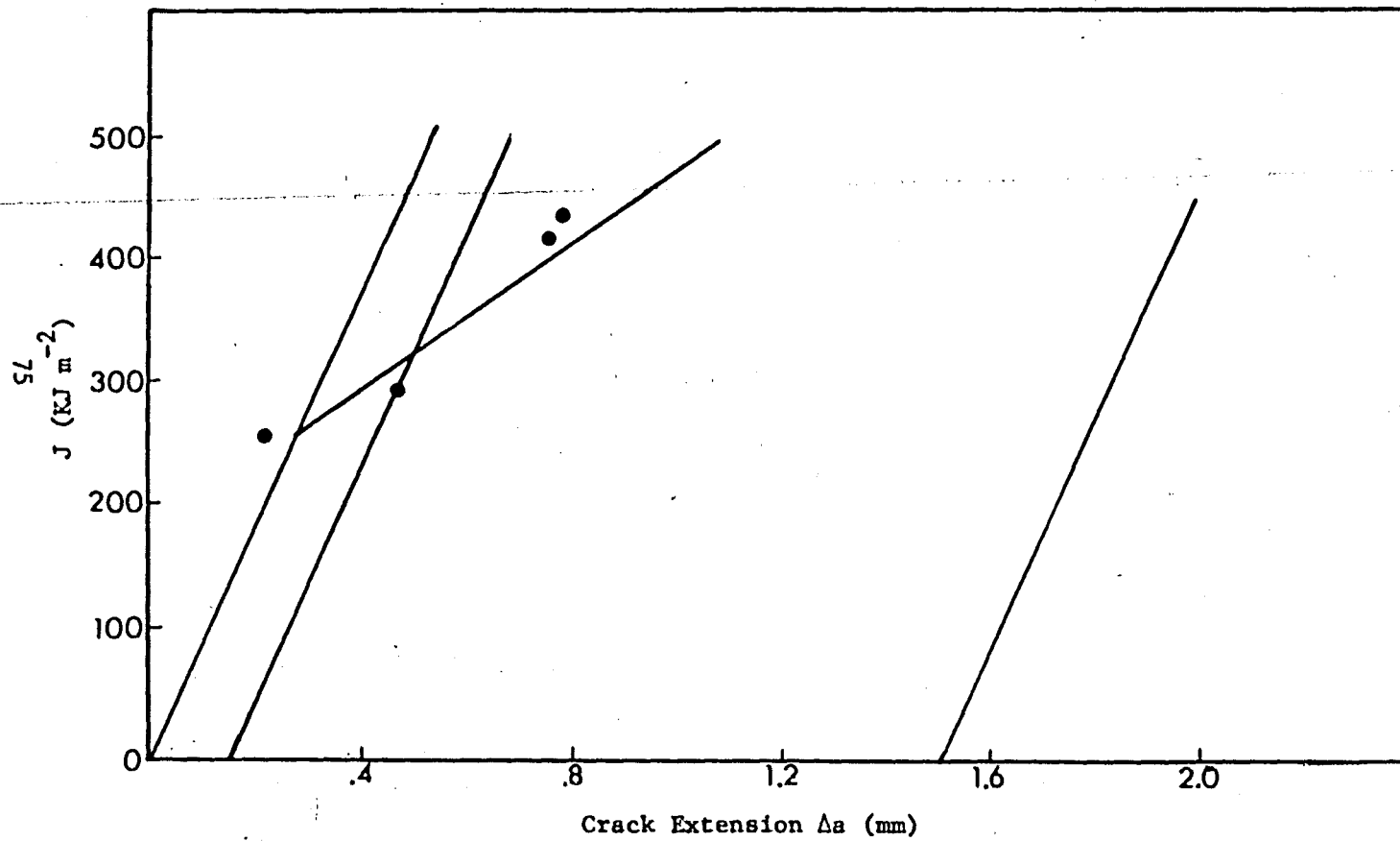FIGURE 17B. CHARPY LATERAL EXPANSION VS. TEMPERATURE ARMCO W-19 WELD METAL STRESS RELIEVED 2 HOURS

72

FIGURE 18A.   CHARPY IMPACT ENERGY VS. TEMPERATURE ARMCO W-19 WELD METAL STRESS RELIEVED 10 HOURS

73

FIGURE 18B. CHARPY LATERAL EXPANSION VS. TEMPERATURE ARMCO W-19 WELD METAL STRESS RELIEVED 10 HOURS

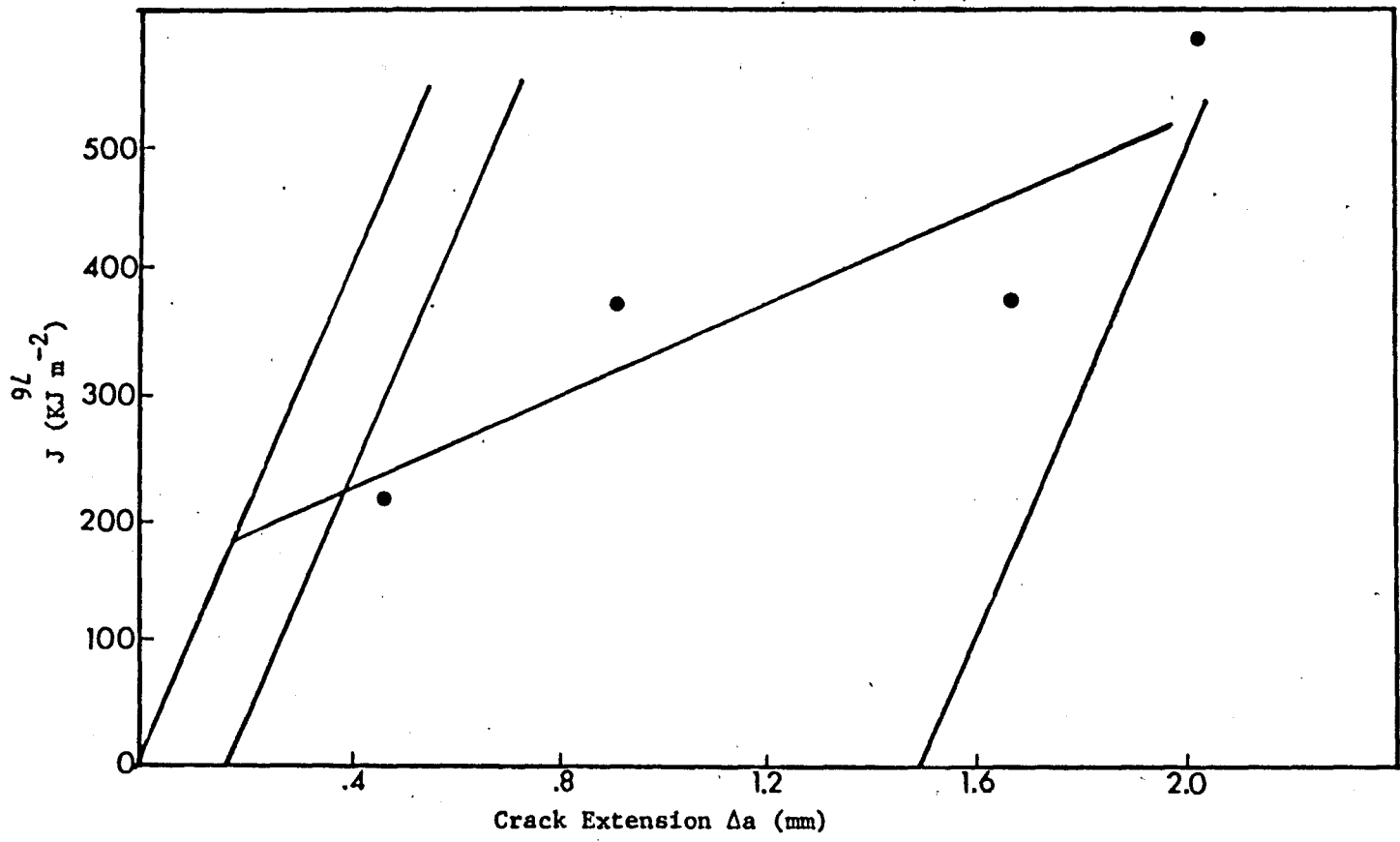FIGURE 19.   J VS. Δa CURVE A737B BASE PLATE 22°C (FROM REFERENCE 2)

FIGURE 20.   J VS. Δa CURVE A737B HAZ AS WELDED: ROOM TEMPERATURE TESTS 22°C
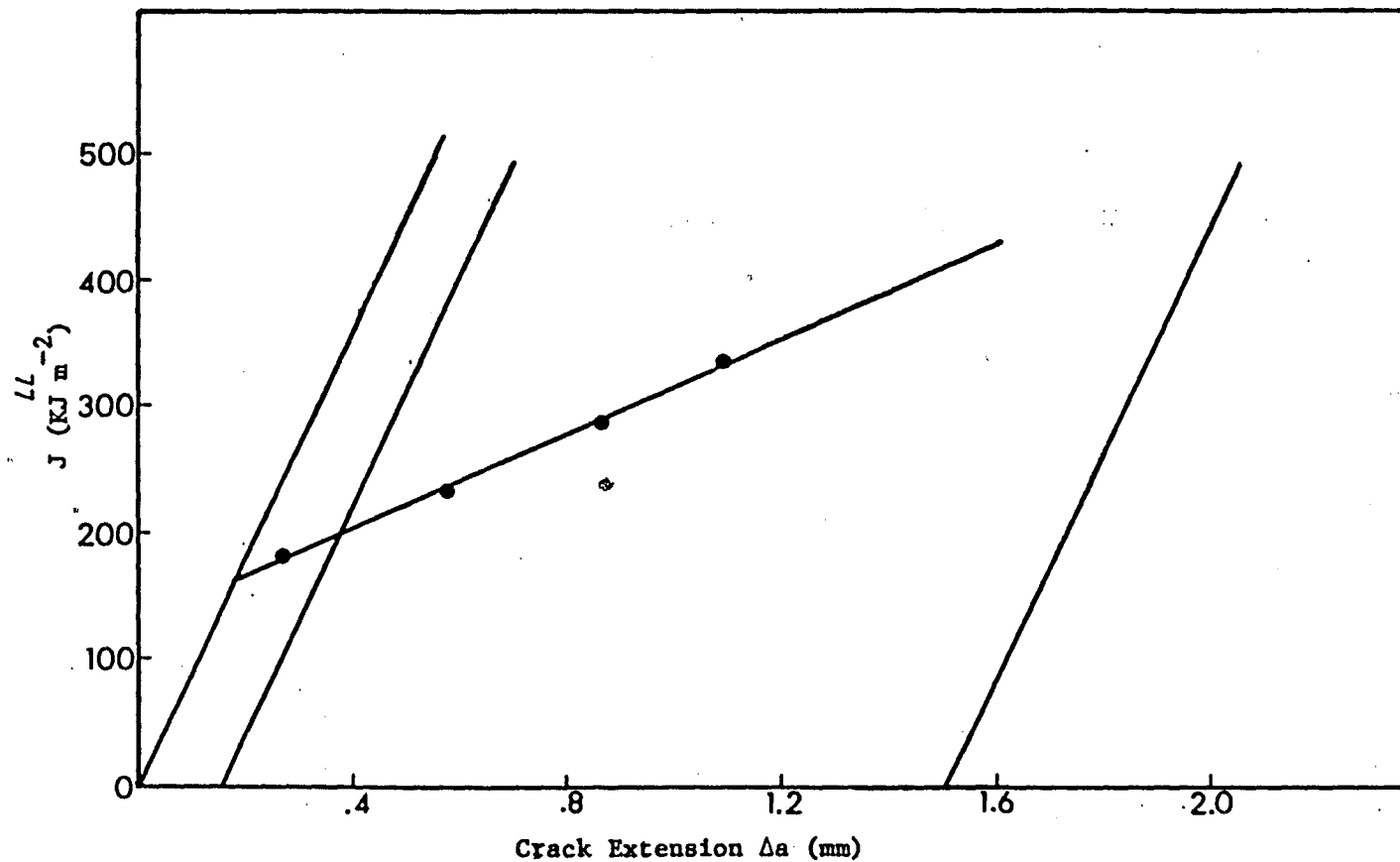
FIGURE 21.   J VS. Δa CURVE A737B STRESS
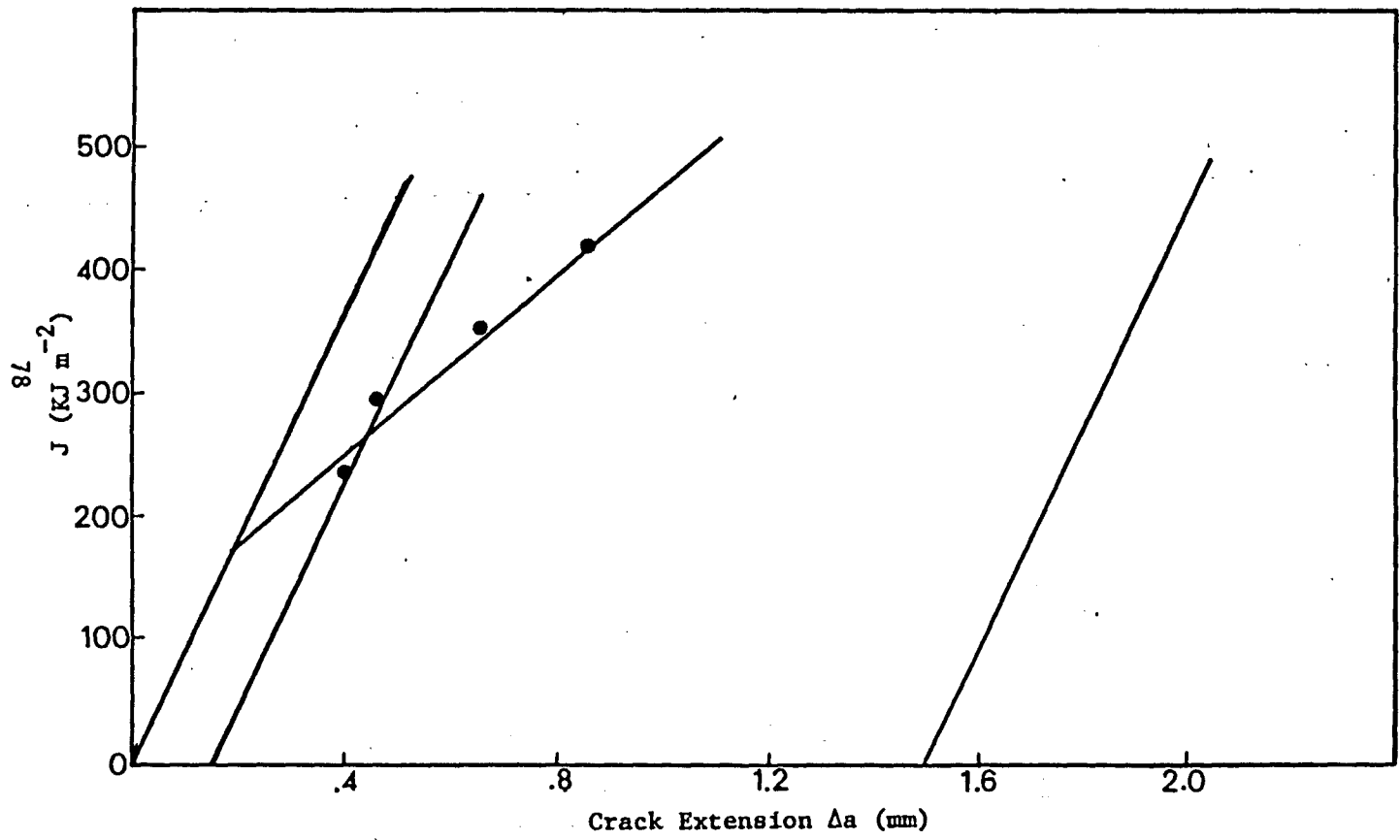RELIEVED 593°C, 2H: ROOM TEMPERATURE TESTS 22°C

FIGURE 22. J VS. Δa CURVE A737B HAZ STRESS
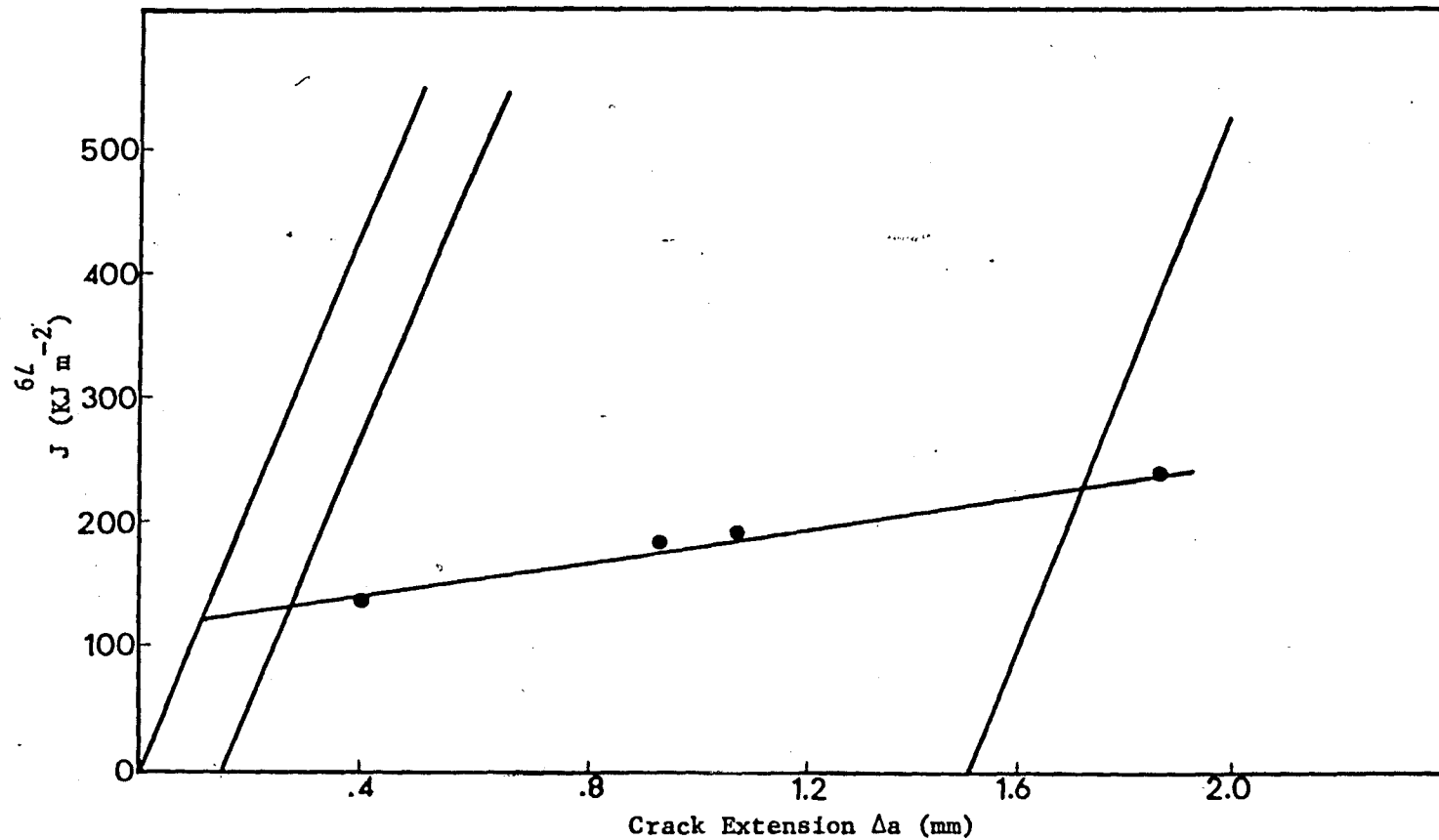RELIEVED 593°C, 10H: ROOM TEMPERATURE TESTS 22°C

FIGURE 23.   J VS. Δa CURVE ARMCO W-19 WELD AS WELDED: ROOM TEMPERATURE TESTS 22°C
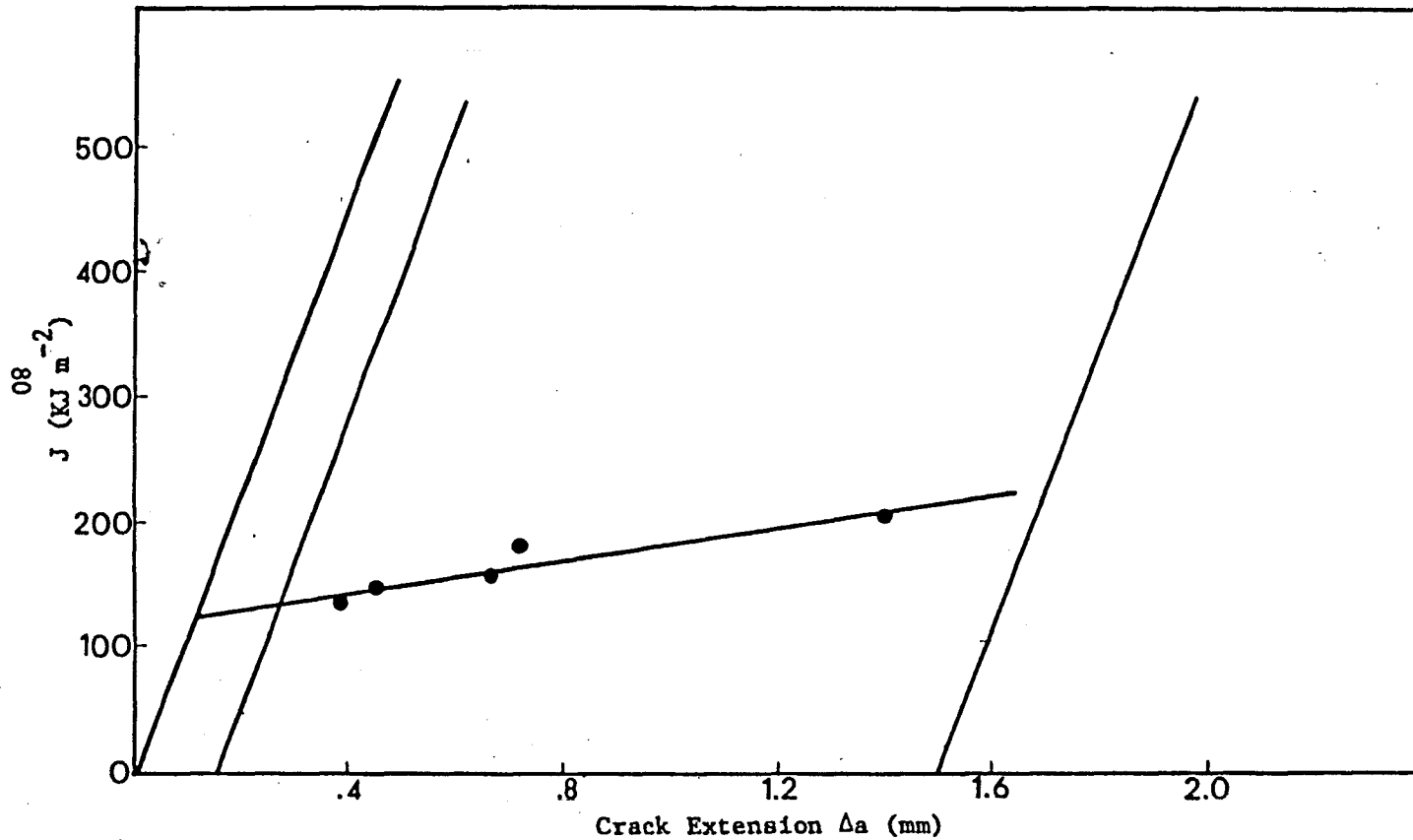
FIGURE 24. J VS. Δa CURVE ARMCO W-19 WELD STRESS RELIEVED 593°C, 2H: ROOM TEMPERATURE TESTS 22°C
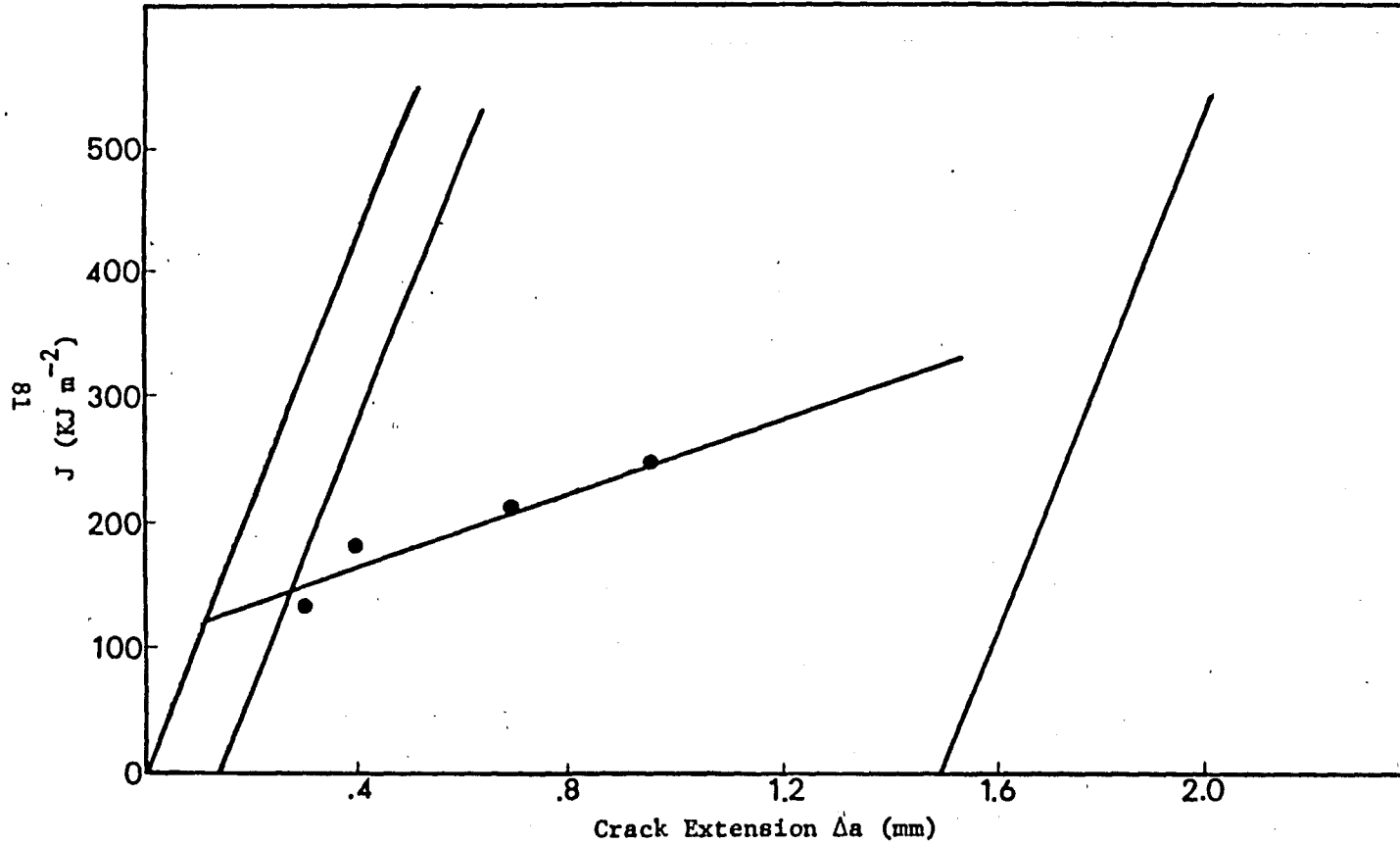
FIGURE 25. J VS. Δa CURVE ARMCO W-19 WELD METAL STRESS RELIEVED 593°C, 10H: 22°C

REFERENCES

1. A. W. Pense, "1980 Adams Lecture: Twenty Years of Pressure Vessel Steel Research", Welding Journal, November 1980, Vol. 59, pp. 311s-325s.

2. J. I. Qureshi, "Static and Dynamic Fracture Behavior of A737 Grade B Steel", October 1978, Master's Thesis, Department of Metallurgy and Materials Engineering, Lehigh University.

3. J. D. Aadland, "Fracture Toughness Behavior of A737 Grade C Pressure Vessel Steel", April 1980, Master's Thesis, Department of Metallurgy and Materials Engineering, Lehigh University.

4. N. Shinohe, "Stress Relief Effects in Nb Containing Microalloyed Steel", May 1979, Master's Thesis, Department of Metallurgy and Materials Engineering, Lehigh University.

5. M. Sekizawa, "The Effect of Strain Aging and Stress Relief Heat Treatment on A737 Grade C Pressure Vessel Steel", September 1981, Master's Thesis, Department of Metallurgy and Materials Engineering, Lehigh University.

6. W. A. Herman, "The Effect of Strain Aging and Stress Relief Heat Treatment of A737 Grade B Pressure Vessel Steel", September 1981, Master's Thesis, Department of Metallurgy and Materials Engineering, Lehigh University.

7. M. S. Rashid, "GM 980 X-A Unique High Strength Sheet Steel With Superior Formability", SAE Paper 760206, Transactions of the Society of Automotive Engineers, Vol. 85, Section 2, 1976, pp. 938-949.

8. D. F. Baxter Jr., "GM Develops a Superformable HSLA Steel", Metal Progress, August 1977, Vol. 112, pp. 44-48.

9. J. H. Bucher and E. C. Hamburg, "High Strength Formable Sheet Steel", SAE Paper 770164, Transactions of the Society of Automotive Engineers, Vol. 86, Section 1, 1977, pp. 730-739.

10. F. B. Pickering, "High-Strength Low-Alloy Steels – A Decade of Progress", Microalloying 75 Proceedings, Conference, Washington, D. C., October 1975, published by Union Carbide Corporation, New York, 1977, pp. 9-30.

11. W. Barr and A.J.K. Honeyman, "Effect of the Manganese/Carbon Ratio on the Brittle Fracture of Mild Steel", Journal of the Iron and Steel Institute, October 1947, Vol. 157, pp. 239-242.

12. E. O. Hall, "The Deformation and Aging of Mild Steel: III Discussion of Results", Proceedings of the Physics Society of London, Section B, Vol. 64, 1951, pp. 747-753.

13. N. J. Petch, "The Cleavage Strength of Polycrystals", Journal of the Iron and Steel Institute, May 1953, Vol. 174, pp. 25-28.

14. F. W. Starrat, "Columbium-Treated Steels Low-Cost, High-Strength", Journal of Metals, December 1958, Vol. 10, p. 799.

15. W. B. Morrison and J. H. Woodhead, "The Influence of Small Niobium Additions on the Mechanical Properties of Commercial Mild Steels", Journal of the Iron and Steel Institute, January 1963, Vol. 201, pp. 43-46.

16. W. B. Morrison, "The Influence of Small Niobium Additions on the Properties of Carbon-Manganese Steels", Journal of the Iron and Steel Institute, April 1963, Vol. 201, pp. 317-325.

17. K. J. Irvine and F. B. Pickering, "Low-Carbon Steels With Ferrite-Pearlite Structures", Journal of the Iron and Steel Institute, November 1963, Vol. 201. pp. 944-959.

18. K. J. Irvine, F. B. Pickering, and T. Gladman, "Grain-Refined C-Mn Steels", Journal of the Iron and Steel Institute, February 1967, Vol. 205, pp. 161-182.

19. J. L. Mihelich, J. R. Bell, and M. Korchynsky, "Effect of Inclusion Shape on the Ductility of Ferritic Steels", Journal of the Iron and Steel Institute, June 1971, Vol. 209, pp. 469-475.

20. L. Luyckx, J. R. Bell, A. McLean, and M. Korchynsky, "Sulfide Shape Control in High Strength Low Alloy Steels", Metallurgical Transactions, December 1970, Vol. 1, pp. 3341-3350.

21. D. C. Hilty and V. T. Popp, "Improving the Influence of Calcium on Inclusion Control", Electric Furnace Proceedings, TMS-AIME, 1969, Vol. 27, pp. 52-66.

22. L. Meyer, F. Heisterkamp, and W. Mueschenborn, "Columbium, Titanium, and Vanadium in Normalized, Thermo-Mechanically Treated and Cold-Rolled Steels", Microalloying 75 Proceedings, Conference, Washington, D. C. October 1975, published by Union Carbide Corporation, New York, 1977, pp. 153-167.

23. E. E. Fletcher, High-Strength Low-Alloy Steels: Status Selection and Physical Metallurgy, Battelle Press, Columbus, Ohio, 1979, pp. 126-129 and 48-64.

24. C. Roper, A. Wilson and C. Entrekin, "Heat Treated Columbium Steel Plate for Low Temperature Applications", Toughness Characterization for HSLA Steels, P. Mangonon editor, TMS-AIME, 1981, pp. 338-360.

25. C. Roper and C. Entrekin, "Metallography of a New Carbon Steel for Low Temperature Service", Metal Progress, February 1981, Vol. 119, pp. 36-41.

26. P. H. M. Hart, R. E. Dolby, N. Bailey, and D. J. Widgery, "The Weldability of Microalloyed Steels", Microalloying 75 Proceedings, Conference, Washington, D.C., October 1975, published by Union Carbide Corporation, New York, 1977, pp. 540-550.

27. R. D. Stout and W. D. Doty, The Weldability of Steel, Third Edition, The Welding Research Council, New York, 1978, pp. 171-189.

28. L. Meyer and H. deBoer, "HSLA Plate Metallurgy: Alloying, Normalizing, Controlled Rolling", Journal of Metals, January 1977, Vol. 29, pp. 17-23.

29. R. E. Dolby, "The Effect of Niobium on the HAZ Toughness of High Heat Input Welds in C-Mn Steels", Welding of HSLA (Microalloyed) Structural Steels, ASM Materials/Metalworking Technology Series, Metals Park, Ohio, 1978, pp. 212-234.

30. N. E. Hannerz, "Weld Metal and HAZ Toughness and Hydrogen Cracking Susceptibility of HSLA Steels as Influenced by Nb, Al, V, Ti, and N", Welding of HSLA (Microalloyed) Structural Steels, ASM Materials/Metalworking Technology Series, Metals Park, Ohio, 1978, pp. 356-401.

31. G. Bernard, "A Viewpoint on the Weldability of Carbon-Manganese and Microalloyed Structural Steels", Microalloying 75 Proceedings, Conference, Washington, D.C., October 1975, published by Union Carbide Corporation, New York, 1977, pp. 552-566.

32. J. R. Rice, "A Path Independent Integral and the Approximate Analysis of Strain Concentration by Notches and Cracks", Journal of Applied Mechanics, Transactions AIME, Vol. 35, 1968, pp. 379-386.

33. J. A. Begley and J. D. Landes, "The J Integral as a Fracture Criterion", Fracture Toughness, ASTM STP 514, 1972, pp. 1-20.

34. J. R. Rice, P. C. Paris, and J. G. Merkle, "Some Further Results of J Integral Analysis and Estimates", Progress in Flaw Growth and Fracture Toughness Testing, ASTM STP 536, 1973, pp. 231-245.

35. J. G. Merkle and H. T. Corten, "A J Integral Analysis for the Compact Specimen Considering Axial Force as Well as Bending Effects", Transactions of the ASME, November 1974, pp. 286-292.

36. J. D. Landes and J. A. Begley, "Recent Developments in J_{1C} Testing", Developments in Fracture Mechanics Test Methods Standardization, ASTM STP 632, 1977, pp. 57-81.

37. G. A. Clarke, W. R. Andrews, J. A. Begley, J. K. Donald, G. T. Embley, J. D. Landes, D. E. McCabe and J. H. Underwood, "A Procedure for the Determination of Ductile Fracture Toughness Values Using J Integral Techniques", Journal of Testing and Evaluation, January 1979, Vol. 7, pp. 49-56.

38. P. C. Paris, J. Tada, A. Zahoor, and H. Ernst, "The Theory of Instability of the Tearing Mode of Elastic-Plastic Crack Growth", Elastic-Plastic Fracture, ASTM STP 668, 1979, pp. 5-36.

39. J. D. Landes and J. A. Begley, "Test Results From J-Integral Studies: An Attempt to Establish a J_{1C} Testing Procedure", Fracture Analysis, ASTM STP 560, 1974, pp. 170-186.

40. P. H. Francis, T. S. Cook, and A. Nagy, "The Effect of Strain Rate on the Toughness of Ship Steels", Ship Structure Committee, SSC 275, 1978.

41. A. K. Shoemaker and S. T. Rolfe, "The Static and Dynamic Low-Temperature Crack-Toughness Performance of Seven Structural Steels", Engineering Fracture Mechanics, June 1971, Vol. 2, pp. 319-339.

42. W. F. Brown, Jr. and J. E. Srawley, Plane Strain Crack Toughness Testing of High Strength Metallic Materials, ASTM STP 410, ASTM Philadelphia, 1966, p. 14.

43. T. Hollstein and J. G. Blauel, "On the Relation of the Crack Opening Displacement to the J Integral", International Journal of Fracture, October 1978, Vol. 14, pp. 385-390.

44. R. Roberts and G. V. Krishna, "An Alternate Measure of Fracture Toughness", Engineering Fracture Mechanics, Number 1, 1977, Vol. 9, pp. 87-93.

VITA

Jose Maria Aurrecoechea.

Born: January 17, 1957 in Manila, Philippines to Florencio and Adela Aurrecoechea.

Education: Bachelor of Science in Chemistry (Minor in Metallurgy) from the Complutense University, Madrid, Spain.